J. Fluid Mech. (2007), *vol.* 579, *pp.* 173–226.
doi:10.1017/S0022112007004880 Printed in the United Kingdom

Electro-osmotic slip and electroconvective instability

B. ZALTZMAN AND I. RUBINSTEIN

DSEEP, Blaustein Institutes for Desert Research, Ben-Gurion University of the Negev, Sede-Boqer Campus, 84990, Israel

(Received 21 July 2006 and in revised form 19 November 2006)

Electric conduction from an electrolyte solution into a charge selective solid, such as ion exchange membrane or electrode, becomes unstable when the electrolyte concentration near the interface approaches zero owing to diffusion limitation. The sequence of events leading to instability is as follows: upon the decrease of the interface concentration, the electric double layer at the interface transforms from its common quasi-equilibrium structure to a different, non-equilibrium one. The key feature of this new structure is an extended space charge added to the usual one of the quasi-equilibrium electric double layer. The non-equilibrium electro-osmotic slip related to this extended space charge renders the quiescent conductance unstable. A unified asymptotic picture of the electric double-layer undercurrent, encompassing all regimes from quasi-equilibrium to the extreme non-equilibrium one, is developed and employed for derivation of a universal electro-osmotic slip formula. This formula is used for a linear stability study of quiescent electric conduction, yielding the precise parameter range of instability, compared with that in the full electroconvective formulation. The physical mechanism of instability is traced both kinematically, in terms of non-equilibrium electro-osmotic slip, and dynamically, in terms of forces acting in the electric double layer.

1. Introduction

In our previous studies of ionic conduction from an electrolyte solution into a charge selective planar solid, such as ion exchange membrane or electrode, we found that this conduction becomes unstable when the electrolyte concentration near the interface approaches zero owing to diffusion limitation (Rubinstein & Zaltzman 2000, 2001, 2003; Rubinstein, Zaltzman & Lerman 2005; Rubinstein *et al.* 2002). The sequence of events leading to instability is as follows: upon the decrease of the interface concentration, the electric double layer (EDL) at the interface transforms from its common quasi-equilibrium structure to a different, non-equilibrium one. The key feature of this new structure is an extended space charge added to the usual one of the quasi-equilibrium EDL. The non-equilibrium electro-osmosis related to this extended space charge renders the quiescent conductance unstable. As a result, a macroscopic vortical electroconvective flow develops which destroys the diffusion layer at the solid/liquid interface. This development, reminiscent of Rayleigh–Bénard and Marangoni instabilities in thermal conduction, may prove useful for intensification of ionic mass transport near the electrodes, design of electrokinetic micro-pumps and desalination by electrodialysis.

Historically, the term electroconvection has been used in at least four different contexts. Thus, this term often refers to the electric-field-induced flow of nematic liquid crystals (Nasumo & Kai 1991; Rehberg, Horner & Hartung 1991; Winkler *et al.* 1991). The same term relates to the flow of liquid dielectrics caused by the action of an electric field on the space charge of ions of the appropriate sign injected into a low quantity into the fluid (see Schneider & Watson 1970; Castellanos & Velarde 1981; Perez & Castellanos 1989). This term is also applied to the effects of an electric field acting on the surface charge accumulated at the interface between two weakly conducting fluids. This mode of electroconvection has been studied by Taylor (1966), who in the mid 1960s introduced the leaky dielectric model to explain the behaviour of droplets deformed by a steady field. This model, extensively used by Melcher (1981), later formed an important step in the construction of a unified treatment of electrohydrodynamics of liquid dielectrics (see Saville 1997).

As opposed to the aforementioned systems, herein (following Grigin 1985; Bruinsma & Alexander 1990; Rubinstein 1991; Baygents & Baldessari 1998; Chen *et al.* 2005; Posner & Santiago 2006), we use the term electroconvection to refer to the flow of strong electrolytes at moderate concentration, that is, to liquids containing many charge carriers of both signs. This type of electroconvection has been invoked, in particular, as a mechanism crucial for over-limiting conductance through cation-exchange electrodialysis membranes (see Rubinstein & Zaltzman 2000) and important for ramified electrodeposition (see Fleury, Chazalviel & Rosso 1993; Fleury, Kaufman & Hibbert 1994; Livermore & Wong 1994) and layering of colloid crystals on electrode surfaces (see Trau, Saville & Aksay 1996, 1997).

The following two modes of electroconvection in strong electrolytes may be distinguished. The first is the relatively recently invoked 'bulk' electroconvection, due to the volume electric forces acting on a macroscopic scale in a locally quasi-electroneutral electrolyte (see Grigin 1985, 1992; Bruinsma & Alexander 1990; Rubinstein, Zaltzman & Zaltzman 1995; Baygents & Baldessari 1998; Buchanan & Saville 1999; Alexandrov, Grigin & Davydov 2002; Lerman, Rubinstein & Zaltzman 2005). The second is the common electro-osmosis, either of the classical 'first' kind or of the 'second' kind, according to Dukhin's terminology (see Dukhin 1991). Electro-osmosis of the 'first' kind (see Dukhin & Derjaguin 1976; Zholkovskij, Vorotyntsev & Staude 1996; Bazant & Squires 2004*a*, *b*) relates to the electrolyte slip resulting from the action of the tangential electric field upon the space charge of a quasi-equilibrium EDL. (The notion of 'induced-charge' electro-osmosis (Bazant & Squires 2004*a*, *b*; Bazant, Thornton & Ajdari 2004) refers to the dependence of the potential drop across quasi-equilibrium EDL, governing the electro-osmotic flow rate, on the applied electric field as opposed to the classical view in which this drop is regarded as a material constant.) Electro-osmosis of the 'second' kind invoked by Dukhin (see Dukhin & Mishchuk 1989; Dukhin, Mishchuk & Takhistov 1989; Mishchuk, Gonzalez-Caballero & Takhistov 2001; Ben & Chang 2002) pertains to the similar action of a tangential electric field upon the extended space charge of the non-equilibrium EDL.

In our previous studies, we developed the theory of non-equilibrium electro-osmotic slip of this kind, valid for extreme non-equilibrium conditions, and showed that this slip causes instability of the quiescent passage of a d.c. electric current from an electrolyte solution into a planar charge selective solid (see Rubinstein & Zaltzman 2000, 2001, 2003; Rubinstein *et al.* 2002, 2005). This instability was of a singular short-wave type: the marginal stability curve in the control parameter (voltage) versus wavenumber plane did not have a minimum, whereas the linear growth rate

increased indefinitely upon the increase of the wavenumber. This suggested the need to look for a regularized formulation and a wavenumber selection criterion. Inclusion of higher-order terms in the limiting formulation provided the necessary regularization (see Rubinstein & Zaltzman 2003). Rubinstein *et al.* (2005) compared linear stability results for the leading-order electro-osmotic formulations with those for the full electroconvective formulation. Developing a universal theory of electro-osmotic slip, uniformly valid for both equilibrium and non-equilibrium conditions, the latter not necessarily of the extreme type considered previously, is the central goal of the present study. Possessing such a theory will allow us to determine the precise parameter ranges of instability of quiescent conduction and to study the resulting nonlinear electroconvective flow. (From our preliminary studies we know that in such a flow which is difficult for direct numerical simulations, quasi-equilibrium and non-equilibrium sections of the interface alternate, rendering the universal slip condition indispensable.)

An experimental test of the electro-osmotic origin of overlimiting conductance is described in Rubinstein *et al.* (2002). In these experiments, a thin fluid layer near the interface was immobilized by an aqueous uncharged solid (cross-linked poly-methyl-alcohol) thus, eliminating electro-osmosis. As a result, overlimiting conductance disappeared.

Our presentation is organized as follows. In § 2, we formulate the general electroconvection problem and review various limiting electro-osmotic formulations. In § 3, we develop a unified description of EDL undercurrent, valid for all regimes from quasi-equilibrium to the extreme non-equilibrium one. In § 4, we employ this description for derivation of a universally valid electro-osmotic slip formula. Next, in § 5, we employ this formula to study the linear stability of quiescent ionic conduction (concentration polarization). In § 6, we compare these linear stability results for the limiting slip formulation with those for the full electroconvection problem and show that the universal slip formula yields a neutral stability curve close to that in the full formulation. Finally, in § 7, we discuss the physical mechanism of the described non-equilibrium electro-osmotic instability.

2. Two types of electroconvection in concentration polarization

The prototypical two-dimensional model problem for ionic conduction in a layer of a univalent electrolyte flanked by two ideally permselective cation-exchange membranes under the passage of a normal electric current (from right to left) in the dimensionless form are given below (see Rubinstein 1990; Rubinstein & Zaltzman 2001) (tiltes are used for the dimensional variables, as opposed to their dimensionless counterparts, see figure 1 for the geometry).

Equations $\{-\infty < x < \infty, \quad 0 < y < 1\}$

$$\frac{\partial c^+}{\partial t} + Pe(\boldsymbol{v}\cdot\nabla)c^+ = \frac{D+1}{2}\nabla\cdot(\nabla c^+ + c^+\nabla\varphi), \tag{2.1}$$

$$\frac{\partial c^-}{\partial t} + Pe(\boldsymbol{v}\cdot\nabla)c^- = \frac{D+1}{2D}\nabla\cdot(\nabla c^- - c^-\nabla\varphi), \tag{2.2}$$

$$\varepsilon^2\Delta\varphi = c^- - c^+, \tag{2.3}$$

$$\frac{1}{Sc}\frac{\partial \boldsymbol{v}}{\partial t} = -\nabla p + \Delta\varphi\nabla\varphi + \Delta\boldsymbol{v}, \tag{2.4}$$

$$\nabla\cdot\boldsymbol{v} = 0. \tag{2.5}$$

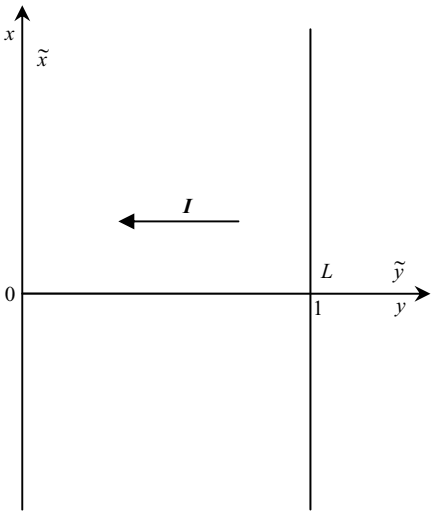

FIGURE 1. Sketch of the geometry of the problem.

The Nernst–Planck equations (2.1) and (2.2) describe convective electrodiffusion of cations and anions, respectively. Equation (2.3) is the Poisson equation for the electric potential, where $c^+ - c^-$ on the right-hand side is the space charge due to a local imbalance of ionic concentrations. The Stokes equation (2.4) is obtained from the full momentum equation by omitting the nonlinear inertia terms. Finally, (2.5) is the continuity equation for an incompressible solution. Spatial variables in (2.1)–(2.5) have been non-dimensionalized with the layer thickness L whereas

$$t = \frac{\widetilde{t} D_0}{L^2}, \quad c^+ = \frac{\widetilde{c}^+}{c^0}, \quad c^- = \frac{\widetilde{c}^-}{c^0}, \quad \varphi = \frac{F\widetilde{\varphi}}{RT}$$

are, respectively, the dimensionless time, concentrations of cations and anions and the electric potential, with c_0 being the typical concentration, e.g. average anion concentration in the layer, F the Faraday constant, R the universal gas constant, T the absolute temperature and the 'salt' diffusivity D_0 defined as

$$D_0 = \frac{2D_+D_-}{D_+ + D_-}$$

where D_+ and D_- are the cationic and anionic diffusivities, respectively. Furthermore, $\boldsymbol{v}$ and p in (2.4), (2.5) are the dimensionless velocity vector and pressure, defined as

$$\boldsymbol{v} = \widetilde{\boldsymbol{v}}/v_0 = u\hat{\boldsymbol{i}} + w\hat{\boldsymbol{j}}, \quad p = \widetilde{p}/p_0,$$

with the typical velocity v_0 and pressure p_0 determined from the force balance in the dimensional version of the momentum equation (2.4) as:

$$v_0 = \frac{d(RT/F)^2}{4\pi\eta L}, \quad p_0 = \frac{\eta v_0}{L},$$

where d is the dielectric constant of the solution and η is the dynamic viscosity of the fluid. Below, we list and discuss the dimensionless parameters in the system (2.1)–(2.5).

(i) The dimensionless Debye length ε is defined as

$$\varepsilon = \frac{(dRT)^{1/2}}{2F(\pi c_0)^{1/2}}. \tag{2.6}$$

ε^2 lies in the range $2\times10^{-13} < \varepsilon^2 < 2\times10^{-5}$, for a realistic macroscopic system with $10^{-4} < L(\text{cm}) < 10^{-1}$, $10^{-4} < c_0(\text{mol}) < 1$.

(ii) The Péclet number Pe is defined as

$$Pe = v_0 L/D_0,$$

or, substituting v_0,

$$Pe = \left(\frac{RT}{F}\right)^2 \frac{d}{4\pi\eta D_0}. \tag{2.7}$$

From (2.7), Pe does not depend on c_0, L and for a typical aqueous low molecular electrolyte is of order unity (more precisely, $Pe \simeq 0.5$).

(iii) Sc is the Schmidt number defined as

$$Sc = \nu/D_0.$$

Here ν is the kinematic viscosity of the fluid.

(iv) The relative cationic diffusivity D is defined as

$$D = D_+/D_-.$$

Boundary conditions

$y = 0$ *(cathode membrane's surface)*

$$\left(\frac{\partial c^-}{\partial y} - c^- \frac{\partial \varphi}{\partial y}\right)\bigg|_{y=0} = 0. \tag{2.8}$$

Condition (2.8) states impermeability for anions of an ideally permselective cation exchange membrane.

$$c^+|_{y=0} = p_1. \tag{2.9}$$

This condition, prescribing interface concentration equal to that of the fixed charges inside the membrane (p_1), is asymptotically valid for $p_1 \gg 1$ and amounts to disregarding the co-ion invasion of an ideally permselective membrane and the presence of an $O\left(\varepsilon/\sqrt{p_1}\right)$ thick boundary layer on the membrane side of the interface

$$\varphi|_{y=0} = -V. \tag{2.10}$$

This condition, valid for the so-called potentiostatic operation, specifies a value V (voltage) potential drop between the membranes; V is the control parameter in our treatment.

$$\boldsymbol{v}|_{y=0} = 0. \tag{2.11}$$

This is the common non-slip condition.

$y = 1$ *(anode membrane's surface)*

$$\left(\frac{\partial c^-}{\partial y} - c^- \frac{\partial \varphi}{\partial y}\right)\bigg|_{y=1} = 0, \quad c^+|_{y=1} = p_1, \quad \varphi|_{y=1} = 0, \quad \boldsymbol{v}|_{y=1} = 0. \tag{2.12a–d}$$

Conditions (2.12*a–d*) are analogous to (2.8)–(2.11). Conditions (2.8)–(2.12*a–d*) are complemented by

$$\lim_{l\to\infty}\frac{1}{2l}\int_{-l}^{l}\int_{0}^{1}c^{-}(x,y)\,\mathrm{d}y\,\mathrm{d}x=1, \tag{2.13}$$

specifying the number of anions in the system. When time-dependent situations are addressed, boundary-value problem (2.1)–(2.5), (2.8)–(2.13) is supplemented by a suitable set of initial conditions.

The boundary-value problem (2.1)–(2.5), (2.8)–(2.13) possesses a one-dimensional quiescent conduction solution with $\boldsymbol{v}=0$, and c^{+}, c^{-} and φ satisfying the relations

$$\frac{\mathrm{d}}{\mathrm{d}y}\left(\frac{\mathrm{d}c^{+}}{\mathrm{d}y}+c^{+}\frac{\mathrm{d}\varphi}{\mathrm{d}y}\right)=0,\quad \frac{\mathrm{d}}{\mathrm{d}y}\left(\frac{\mathrm{d}c^{-}}{\mathrm{d}y}-c^{-}\frac{\mathrm{d}\varphi}{\mathrm{d}y}\right)=0, \tag{2.14a,b}$$

$$\varepsilon^{2}\frac{\mathrm{d}^{2}\varphi}{\mathrm{d}y^{2}}=c^{-}-c^{+}, \tag{2.15}$$

$$\left(\frac{\mathrm{d}c^{-}}{\mathrm{d}y}-c^{-}\frac{\mathrm{d}\varphi}{\mathrm{d}y}\right)\Big|_{y=0,1}=0,\quad c^{+}|_{y=0,1}=p_{1},\quad \int_{0}^{1}c^{-}(x,y)\,\mathrm{d}y=1, \tag{2.16a–c}$$

$$\varphi|_{y=1}=0,\quad \varphi|_{y=0}=-V, \tag{2.17a,b}$$

and

$$p(y)=\frac{1}{2}\left(\frac{\mathrm{d}\varphi}{\mathrm{d}y}\right)^{2}+p_{c}, \tag{2.18}$$

where p_c is an arbitrary integration constant.

For quasi-equilibrium conditions, the solution of boundary-value problem (2.14a,b)–(2.17a,b) splits into the 'outer' locally electroneutral solution, valid in the 'bulk' of the segment $0<y<1$, and the 'inner' or EDL solutions, valid in the ε-vicinity of the interfaces at $y=0,1$ (see Rubinstein 1990; Rubinstein & Zaltzman 2000). The inner and outer solutions are connected through the standard procedures of matched asymptotic expansions. The outer leading-order solution is that to the quasi-electroneutral boundary-value problem:

$$\frac{\mathrm{d}}{\mathrm{d}y}\left(\frac{\mathrm{d}\overline{c}}{\mathrm{d}y}+\overline{c}\,\frac{\mathrm{d}\overline{\varphi}}{\mathrm{d}y}\right)=0,\quad \frac{\mathrm{d}}{\mathrm{d}y}\left(\frac{\mathrm{d}\overline{c}}{\mathrm{d}y}-\overline{c}\,\frac{\mathrm{d}\overline{\varphi}}{\mathrm{d}y}\right)=0\qquad (0<y<1), \tag{2.19a,b}$$

$$\left(\frac{\mathrm{d}\overline{c}}{\mathrm{d}y}-\overline{c}\,\frac{\mathrm{d}\overline{\varphi}}{\mathrm{d}y}\right)\Big|_{y=0,1}=0,\quad (\ln\overline{c}+\overline{\varphi})|_{y=0}=\ln p_{1}-V, \tag{2.20a,b}$$

$$(\ln\overline{c}+\overline{\varphi})|_{y=1}=\ln p_{1},\quad \int_{0}^{1}\overline{c}(y)\,\mathrm{d}y=1. \tag{2.21a,b}$$

Here

$$\overline{c}\overset{\text{def}}{=}c^{+}=c^{-},$$

and conditions (2.20b) and (2.21a) express the continuity of the electrochemical potential of cations (capable of penetrating the interfaces at $y=0,1$) across the discontinuities of the electric potential and ionic concentration, modelling the EDL in the outer problem. The outer (quiescent concentration polarization) solution is

obtained by a straightforward integration of the boundary-value problem (2.19*a*, *b*)–(2.21*a*, *b*) in the form

$$\overline{c}(y) = \frac{I}{2}\left(y - \tfrac{1}{2}\right) + 1, \quad \overline{\varphi}(y) = \ln\left[\frac{I}{2}\left(y - \tfrac{1}{2}\right) + 1\right] + \ln\frac{p_1}{(1 + I/4)^2}, \tag{2.22a, b}$$

where

$$I \overset{\text{def}}{=} \frac{\mathrm{d}\overline{c}}{\mathrm{d}y} + \overline{c}\frac{\mathrm{d}\overline{\varphi}}{\mathrm{d}y} \tag{2.23}$$

is the electric current density in the system. Equation (2.23) yields the current–voltage relation

$$I = 4\frac{1 - \mathrm{e}^{-V/2}}{1 + \mathrm{e}^{-V/2}}. \tag{2.24}$$

From (2.24), when $V \to \infty$, $I \to I^{lim} = 4$ and, simultaneously, by equations (2.22*a*, *b*), $\overline{c}(0) \to 0$ and

$$\lim_{y \to 0} \frac{\overline{\varphi}}{\ln y} = 1. \tag{2.25}$$

This is the key feature in the classical picture of concentration polarization – saturation of the current density towards the limiting value, resulting from the vanishing interface electrolyte concentration and the development of logarithmic singularity of electric potential at the cathode. In fact, currents much greater than the limiting one are readily passed through virtually ideally permselective cation-exchange membranes (overlimiting conductance mentioned in § 1). Search for a mechanism for this and the related occurrence of the excess electric noise, provided the main motivation for our study of electroconvection in strong electrolytes. (In real systems electroconvection is superimposed upon gravitational convection owing to density variation induced by concentration changes and Joule heating, enhanced near the depleted interface. Moreover, in the absence of forced convection, large-scale gravitational flow is the major factor determining the parameters of the diffusion layer at the solution/solid interface. On the other hand, the thickness of this layer is usually too small – tens to a few hundred micrometres – for the gravitational convection to become a major factor in the description of the diffusion layer. Moreover, overlimiting conductance is observed in small horizontal polarization cells with gravitationally stable density stratification induced by the electric current (Maletzki, Rosler & Staude 1992; Rubinstein, Shtaude & Kedem 1988; Rubinstein *et al.* 2002.) In order to investigate the stability of the quiescent concentration polarization solution (2.22*a*, *b*)–(2.24), we must allow for lateral motions. In this case too, the problem splits into those for locally quasi-electroneutral bulk and the boundary (electric double) layer at the membrane/solution interface. Equations describing the ionic transfer and fluid flow in the bulk are (see Rubinstein 1991):

$$\frac{\partial\overline{c}}{\partial t} + Pe(\overline{\boldsymbol{v}}\cdot\nabla)\overline{c} = \frac{D+1}{2}\nabla\cdot(\nabla\overline{c} + \overline{c}\nabla\overline{\varphi}), \tag{2.26}$$

$$\frac{\partial\overline{c}}{\partial t} + Pe(\overline{\boldsymbol{v}}\cdot\nabla)\overline{c} = \frac{D+1}{2D}\nabla\cdot(\nabla\overline{c} - \overline{c}\nabla\overline{\varphi}), \tag{2.27}$$

$$\frac{1}{Sc}\frac{\partial\overline{\boldsymbol{v}}}{\partial t} = -\nabla\overline{p} + \Delta\overline{\varphi}\nabla\overline{\varphi} + \Delta\overline{\boldsymbol{v}}, \tag{2.28}$$

$$\nabla\cdot\overline{\boldsymbol{v}} = 0, \tag{2.29}$$

whereas the boundary-layer analysis provides, in addition to boundary conditions (2.20a, b), (2.21a), an expression for electro-osmotic slip, that is the tangential fluid velocity at the outer edge of the EDL. Disregarding this, and assuming non-slip at the solid wall instead, yields the bulk electroconvection formulation, for which a long-time controversy existed with regard to the stability of the one-dimensional quiescent concentration polarization solution (2.22a, b) (see Grigin 1985, 1992; Bruinsma & Alexander 1990; Rubinstein *et al.* 1995; Baygents & Baldessari 1998; Buchanan & Saville 1999; Alexandrov *et al.* 2002). Lerman *et al.* (2005) have shown that for bulk electroconvection this solution is stable. Moreover, it was shown in Rubinstein *et al.* (2005) that the electric force term in (2.28) always has a stabilizing effect on the instability due to non-equilibrium electro-osmosis.

As for the electro-osmotic slip at a conductive permselective interface, two fundamentally different regimes are to be distinguished in accordance with the magnitude of the electric current through the interface and the related state of the EDL. The first, quasi-equilibrium electro-osmosis, or electro-osmosis of the first kind, following terminology of Dukhin (1991), pertains to currents, below the limiting value. For such currents, the diffuse part of the EDL preserves its common quasi-equilibrium structure as essentially identical with that for zero current. For such conditions, the inner problem is reduced to the Poisson–Boltzmann equation

$$\frac{\partial^2\varphi}{\partial z^2} = \overline{c}(x,0,t)\left(\exp(\varphi-\overline{\varphi}(x,0,t))-\exp(-\varphi+\overline{\varphi}(x,0,t))\right). \tag{2.30}$$

Here, $z = y/\varepsilon$ is the cathodic boundary-layer coordinate (correspondingly, $z = (1-y)/\varepsilon$ for the anodic boundary layer), $\varphi(x, z, t)$ is the EDL potential. Solution of (2.30) yields

$$\varphi(x,z,t) = \overline{\varphi}(x,0,t) + 2\ln\frac{\exp(\zeta_q/2)+1+(\exp(\zeta_q/2)-1)\exp(-z\sqrt{2\overline{c}(x,0,t)})}{\exp(\zeta_q/2)+1-(\exp(\zeta_q/2)-1)\exp(-z\sqrt{2\overline{c}(x,0,t)})}. \tag{2.31}$$

Here $\overline{c}(x,0,t)$, $\overline{\varphi}(x,0,t)$ are, respectively, the electrolyte concentration and the electric potential at the outer edge of the EDL and

$$\zeta_q(x,t) = \varphi(x,0,t) - \overline{\varphi}(x,0,t)$$

is the potential drop across the latter.

Theory of quasi-equilibrium electro-osmosis at a permselective interface was developed by Dukhin & Derjaguin (1976). An essential part of this theory is accounting for polarization of the EDL by the applied tangential electric field, resulting, in particular, in major lateral pressure drops in the double layer, owing to the lateral variation of the Maxwell stresses. This results, for the tangential velocity u in the double layer, in the equation of the form

$$-\frac{1}{2}\frac{\partial}{\partial x}\left[\left(\frac{\partial\varphi}{\partial z}\right)^2\right] + \frac{\partial\varphi}{\partial x}\frac{\partial^2\varphi}{\partial z^2} + \frac{\partial^2 u}{\partial z^2} = 0. \tag{2.32}$$

Note that the total lateral electric force in the EDL

$$F_x \overset{\text{def}}{=} \int_0^\infty \frac{\partial\varphi}{\partial x}\frac{\partial^2\varphi}{\partial z^2}\mathrm{d}z \tag{2.33}$$

is equal to minus the total lateral pressure gradient

$$P_x \overset{\text{def}}{=} \int_0^\infty \frac{\partial p}{\partial x}\,\mathrm{d}z. \tag{2.34}$$

Indeed, by (2.18) and (2.34)

$$P_x = \frac{\partial \varphi}{\partial x}\frac{\partial \varphi}{\partial z}\bigg|_{z=0}^{z=\infty} - F_x, \tag{2.35}$$

and because of the vanishing of the boundary term in (2.35) (stabilization at $z=\infty$ and constant potential at $z=0$), we obtain

$$P_x = -F_x. \tag{2.36}$$

Integration of (2.32) with (2.31) yields for the electro-osmotic slip velocity, instead of the common Helmholtz–Smoluchowski formula

$$u_s = \zeta_q \frac{\partial \overline{\varphi}}{\partial x}, \tag{2.37}$$

the expression

$$u_s = \zeta_q \left(\frac{\partial \overline{\varphi}}{\partial x} + \frac{1}{\overline{c}}\frac{\partial \overline{c}}{\partial x} \right) - 4\frac{1}{\overline{c}}\frac{\partial \overline{c}}{\partial x} \ln \frac{1+\mathrm{e}^{\zeta_q/2}}{2}. \tag{2.38}$$

The peculiarity of (2.38) is that, for an ideally permselective cation exchange membrane maintained at a constant potential $\ln \overline{c} + \overline{\varphi} = \text{const}$, that is, $\partial \overline{c}/\partial x = -\overline{c}\partial \overline{\varphi}/\partial x$ and for $\zeta_q \to -\infty$, equation (2.38) yields

$$u_s = -(4 \ln 2)\overline{\varphi}_x. \tag{2.39}$$

That is, the factor at $-\partial \overline{\varphi}/\partial x$ (electro-osmotic factor) tends to a maximal upper value upon the increase of ζ_q (negative). This is in contrast to the respective prediction of Helmholtz–Smoluchowski formula, (2.37), and is a direct consequence of polarization of the EDL at a permselective interface.

Hydrodynamic stability of the quiescent concentration polarization with a limiting quasi-equilibrium electro-osmotic slip, (2.39), was studied in Zholkovskij *et al.* (1996). It was concluded that quasi-equilibrium electro-osmotic instability, although possible in principle near the limiting current, was unfeasible for any realistic low-molecular aqueous electrolyte. This conclusion followed because an electro-osmotic factor at least one order of magnitude higher than the limiting value $4(\ln 2)$ is required for this type of instability to occur. This conclusion is valid as long as the system, in particular, the EDL remains at quasi-equilibrium. This ceases to be the case at the cathodic membrane ($y=0$) when the current approaches the limiting value. We have already seen that in this case, $\overline{c} \to 0$ and $\overline{\varphi} \to -\infty$, which makes (2.30) formally unsuitable for calculation of φ in the EDL and, thus, through (2.32), for calculation of electro-osmotic velocity u_s. This reflects a fundamental structural change which occurs in the system as it moves away from quasi-equilibrium upon $I \to I^{lim}$. The essence of this change is that the division of the system into a locally quasi-electroneutral bulk and a quasi-equilibrium boundary layer breaks down upon $I \to I^{lim}$, as reflected, in particular, in the inconsistency of the local electroneutrality approximation which appears in the basic concentration polarization solution, (2.22*a*, *b*), in this limit.

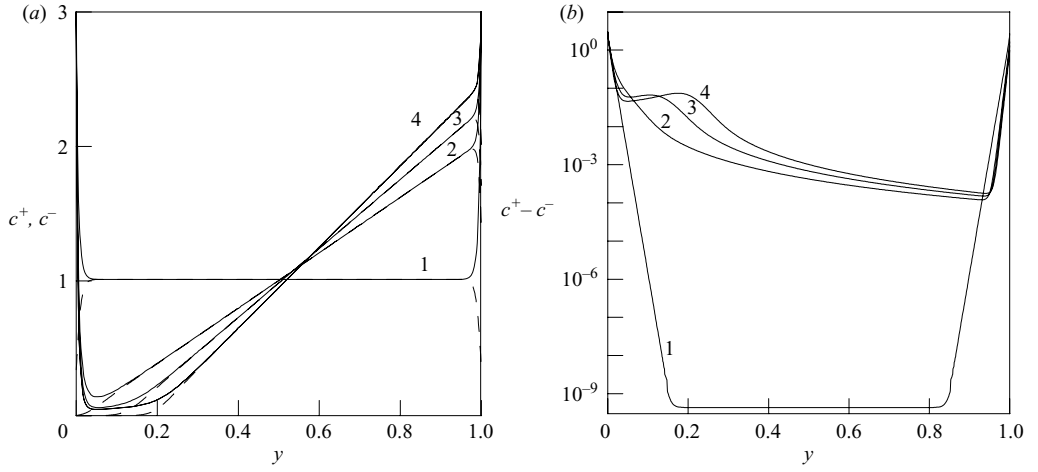

FIGURE 2. (*a*) Ionic concentration profiles (—, c^+; - - -, c^-) for $\varepsilon = 10^{-2}$ and four values of voltage: 1, $V = 0$; 2, $V = 7$; 3, $V = 15$; 4, $V = 20$. (*b*) Space charge density ($c^+ - c^-$) profile for $\epsilon = 10^{-2}$ and four values of voltage: 1, $V = 0$; 2, $V = 7$; 3, $V = 15$; 4, $V = 20$.

Indeed, according to (2.22*b*)

$$\frac{\partial^2 \varphi}{\partial y^2}(0) = \frac{4I^2}{(4-I)^2} \to \infty \quad \text{when } I \to I^{lim} = 4. \tag{2.40}$$

This implies that for any finite ε, however small, setting the left-hand side of the Poisson equation (2.3) equal to zero becomes inconsistent. This breakdown, first notified by Levich (1962) and reflecting the breakdown of the straightforward asymptotic representation of the diffusion layer as a combination of electroneutral bulk and an $O(\varepsilon)$ thick EDL, has motivated several studies of the space charge of the non-equilibrium EDL (see Grafov & Chernenko 1962; Smyrl & Newman 1967; Buck 1973). The picture of the non-equilibrium EDL that emerged from a numerical solution of the one-dimensional problem similar to (2.14*a*, *b*)–(2.18) (see Rubinstein & Shtilman 1979) and which was subsequently confirmed and elaborated by several numerical and analytic studies (see Listovnichy 1989; Nikonenko, Zabolotsky & Gnusin 1989; Manzanares *et al.* 1993; Rubinstein & Zaltzman 2001), may be summarized as follows (see figures 2, 3).

For $0 < V = O(1)$ ($I < I^{lim}$), local electroneutrality holds in the entire system except for the boundary layers of the order of thickness ε at the edges of the region. In the respective electroneutral region, a linear ionic concentration profile holds in accordance with (2.22*a*). The maximal slope of the concentration profile in these conditions is 2, which corresponds to $I = I^{lim}$. This picture remains essentially valid up to $V = O(|\ln \varepsilon|)$ ($I \leqslant I^{lim}$). For $O(|\ln \varepsilon|) < V < O(\varepsilon^{-1})$ ($I \approx I^{\lim}$), the following three regions may be distinguished in the left-hand half-layer (from right to left). The quasi-electroneutral 'bulk' region with a linear concentration profile with a slope of approx twice unity. This region borders on the left with the extended diffuse space charge region of width between $O(\varepsilon^{2/3})$ and $O(1)$, followed by the quasi-equilibrium, $O(\varepsilon)$ thick, boundary layer at the left-hand edge. Upon a further increase of the voltage up to $O(\varepsilon^{-1})$, the extended space charge region reaches a finite size $O(1)$ and so does the current increment over the limiting value [$0 < I - I^{lim} = O(1)$].

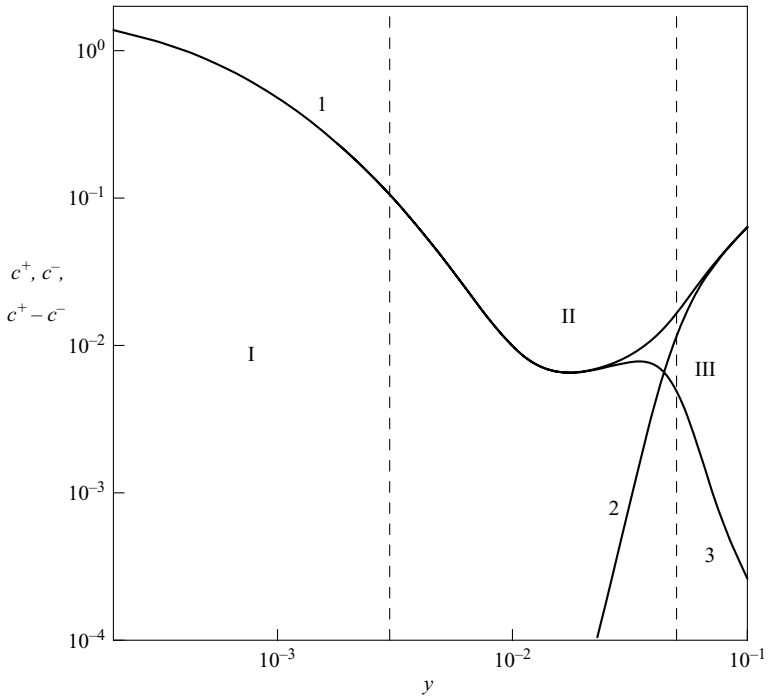

FIGURE 3. Structure of the non-equilibrium boundary layer: I, quasi-equilibrium boundary layer; II, extended space charge region; III, transition layer to quasi-electroneutral bulk. 1, cation concentration c^+; 2, anion concentration c^-; 3, space charge density $(c^+ - c^-)$. $\varepsilon = 10^{-3}$, $V = 20$.

The study of the non-equilibrium EDL has continued since Levich (1962) (see Chu & Bazant 2005 and references therein). Thus, Grafov & Chernenko (1962) undertook the first analytic study of the EDL under current; Smyrl & Newman (1967) focused on what later proved to be the crucial transition mode from the quasi-equilibrium to the non-equilibrium EDL; Rubinstein & Shtilman (1979) identified a suitable model problem, whose solution provided the entire picture of the non-equilibrium EDL, with its extended space charge region, as a part of the macroscopic diffusion layer. Still, no unified description of the EDL under current existed, valid for all regimes from quasi-equilibrium to the extreme non-equilibrium one. In this paper, we finalize such a description based on a systematic asymptotic analysis of a canonical one-dimensional problem extracted from (2.14*a*, *b*)–(2.17*a*, *b*).

The observation of the development in the course of concentration polarization of a non-equilibrium EDL with the extended space charge region lead Dukhin and his colleagues (see Dukhin & Mishchuk 1989; Dukhin *et al.* 1989; Dukhin 1991 and references therein) to conjecture the existence of related non-equilibrium electrokinetic phenomena which they termed electrokinetic phenomena of the second kind.

An accurate analysis of non-equilibrium electro-osmotic slip at a flat permselective membrane for $V > O(|\ln \varepsilon|)$, was carried out in Rubinstein & Zaltzman (2001), resulting in the expression

$$u_s = -\tfrac{1}{8} V^2 \, \frac{\partial}{\partial x} \ln \left. \frac{\partial \overline{c}}{\partial y} \right|_{y=0} . \tag{2.41}$$

Derivation of (2.41) employed the asymptotic theory of the non-equilibrium EDL, previously developed by Listovnichy (1989), and amounted to carrying out an analysis similar to that outlined above for quasi-equilibrium electro-osmosis. Taking account of polarization proved to be more necessary here, since a large potential drop between the membrane surface and the bulk was concerned, that is, namely those conditions for which saturation of the electro-osmotic factor occurred for a quasi-equilibrium electro-osmotic slip. For obtaining a better physical insight into (2.41), it is worth noting that $\partial\overline{c}/\partial y|_{y=0}$ is one half current density through the membrane which is the local characteristic controlling the thickness of the non-equilibrium EDL and, thus, the electric field in it. The accurate analysis of the EDL and its unified description valid for all regimes (§ 3) yield a universal electro-osmotic slip condition (§ 4) and provide us with a limiting electroconvective formulation (§ 5), thus, paving the way for determining the exact thresholds of non-equilibrium electro-osmotic instability (§ 6) and the study of nonlinear electroconvection, in general, and overlimiting conductance, in particular.

3. Unified description of electric double layer undercurrent

The basic idea of our analysis is that there always exists in the vicinity of a planar membrane with constant properties and fixed constant electric potential and counter-ion concentration, a quasi-one-dimensional layer (Q1DL), into which the EDL is embedded, and whose maximal thickness depends on the characteristics of the lateral transport away from the membrane, in particular, the maximal flow velocity and its related Péclet number. We know from our previous studies (see Rubinstein & Zaltzman 2000, 2001) that this Q1DL is of the order of $1/|\ln\varepsilon|$, that is much thicker than any realistic electric double layer of either the equilibrium or non-equilibrium kind. We are about to solve the one-dimensional transport equations in this sublayer and match the obtained solution with that in the two-dimensional quasi-electroneutral bulk (QEB). As will be shown below, the possibility of such a matching is provided by the overlap of the Q1DL with the QEB (Q1DL $\cap$ QEB). From this analysis, a boundary condition for the two-dimensional outer QEB problem will result, depending on a single parameter obtained from the solution of the one-dimensional problem in the Q1DL. There are only two opposite limit cases for which the outer problem decouples completely from that in the Q1DL. Those are the case of the quasi-equilibrium EDL, occurring for electric current below the limiting value, and the case when the extended space charge region of the non-equilibrium EDL is larger by an order of magnitude than $\varepsilon^{2/3}$. In all physically relevant intermediate regimes the coupling of the two problems is essential.

3.1. *One-dimensional analysis in the Q1DL* $\quad 0 < y < O(1/|\ln\varepsilon|)$

Below we consider a thin vicinity of the cathode-exchange the membrane ($0 < y < O[1/|\ln\varepsilon|]$), assuming that the right-hand edge of the considered interval lies in the electroneutral bulk. We distinguish two sublayers in the Q1DL. The first sublayer is the EDL. It will be shown below that, generally, the width of the EDL changes from $O(\varepsilon)$, for potential drops of the order of $O(1)$, to $O(1)$ for very high potential drops of the order of $O(1/\varepsilon)$, irrelevant in the current context. The second portion is the overlap zone of the Q1DL with the QEB. With a natural scaling, the leading-order one-dimensional problem for ionic transport in the Q1DL, written in the original dimensionless variables, is as follows (see Rubinstein & Zaltzman 2001; Rubinstein *et al.* 2005).

Equations

$$\frac{\mathrm{d}c^+}{\mathrm{d}y} + c^+\frac{\mathrm{d}\varphi}{\mathrm{d}y} = I, \quad \frac{\mathrm{d}c^-}{\mathrm{d}y} - c^-\frac{\mathrm{d}\varphi}{\mathrm{d}y} = 0, \quad \varepsilon^2\frac{\mathrm{d}^2\varphi}{\mathrm{d}y^2} = c^- - c^+. \tag{3.1a–c}$$

Boundary conditions at the membrane surface

$$\varphi(x,0,t) = -V, \qquad c^+(x,0,t) = p_1. \tag{3.2a, b}$$

Boundary conditions at the outer edge of the Q1DL

$$c^+ = c^- = \bar{c}, \qquad \ln c^- - \varphi = \mu^- = \mu^-(x,0,t). \tag{3.3a, b}$$

Here, $I(x,t) \overset{\text{def}}{=} i(x,0,t) = 2\bar{c}_y(x,0,t)$, which is the boundary value of the electric current density in the QEB and, correspondingly, the current density independent of y in the Q1DL, $\mu^-(x,y,t)$ is the electrochemical potential of co-ions, also constant in the Q1DL by (3.1*b*).

Equations (3.1*a–c*) may be rewritten as follows

$$\varepsilon\frac{\mathrm{d}}{\mathrm{d}y}(c^+ - c^-) = E(c^+ + c^-) + \varepsilon I \quad (0 < y < O[1/|\ln\varepsilon|]), \tag{3.4}$$

$$\varepsilon\frac{\mathrm{d}c^+}{\mathrm{d}y} = Ec^+ + \varepsilon I, \qquad \varepsilon\frac{\mathrm{d}E}{\mathrm{d}y} = c^+ - c^-, \tag{3.5a, b}$$

where

$$E = -\varepsilon\frac{\mathrm{d}\varphi}{\mathrm{d}y}. \tag{3.6}$$

By substituting (3.5*a, b*) into (3.4) and integrating the resulting equation, we obtain

$$c^+ = \frac{\varepsilon}{2}\frac{\mathrm{d}E}{\mathrm{d}y} + \tfrac{1}{4}E^2 + \frac{I}{2}(y - y_0). \tag{3.7}$$

Here, y_0 is an integration constant.

Considering (3.5*a, b*) in the electroneutral part of the Q1DL and keeping the leading terms in (3.7), we conclude that

$$c^+ = c^- = \bar{c} = \frac{I}{2}(y - y_0) \text{ in Q1DL} \cap \text{QEB}. \tag{3.8}$$

Thus, y_0 is the root of the linear extrapolation of the outer (QEB) ionic concentration profile near the interface. By substituting (3.7) into (3.5*a*), we obtain the following inhomogeneous Painleve equation of the second kind for E

$$\varepsilon^2\frac{\mathrm{d}^2E}{\mathrm{d}y^2} = \tfrac{1}{2}E^3 + I(y - y_0)E + \varepsilon I. \tag{3.9}$$

Seeking an outer asymptotic solution of (3.9) as a power expansion in ε, we find that

$$E = -\frac{\varepsilon}{y - y_0} - \frac{3\varepsilon^2}{2I(y - y_0)^4} + \cdots \quad \text{for } y - y_0 \gg \varepsilon^{2/3}, \tag{3.10}$$

We note that this outer solution is valid for Q1DL $\cap$ QEB that is for y in the range $y - y_0 \gg O(\varepsilon^{2/3})$, $y < O(1/|\ln\varepsilon|)$, with $|c^+ - c^-| \ll O(\varepsilon^{2/3})$ and $|\varphi_y| \leqslant O(\varepsilon^{-2/3})$. Integration of the asymptotic expansion (3.10) in Q1DL $\cap$ QEB and (3.8) yields to the leading order

$$\varphi(x,y,t) = \ln(y - y_0) + \Phi(x,t) = \overline{\varphi} \text{ in Q1DL} \cap \text{QEB}, \tag{3.11}$$

where

$$\Phi(x,t) \stackrel{\text{def}}{=} \ln\frac{I}{2} - \mu^{-}(x,0,t) = \phi(x,0,t). \tag{3.12}$$

Another constant in the Q1DL, is the boundary value of the regular component of the electric potential in the QEB, defined as

$$\phi(x,y,t) \stackrel{\text{def}}{=} \overline{\varphi}(x,y,t) - \ln(y-y_0). \tag{3.13}$$

The representation (3.13) reflects the very essence of concentration polarization at the limiting current (see (2.25)).

To analyse (3.9), we define the boundary-layer variables F and z by the equalities

$$E = I^{1/3}\varepsilon^{1/3}F, \qquad y = I^{-1/3}\varepsilon^{2/3}z. \tag{3.14a,b}$$

In terms of these variables, the boundary-value problem (3.9), (3.2a,b), (3.3a,b), (3.11–3.13) is transformed into

$$\frac{\mathrm{d}^2F}{\mathrm{d}z^2} = \tfrac{1}{2}F^3 + (z-z_0)F + 1 \quad \left(0 < z < O(\varepsilon^{-2/3}/|\ln(\varepsilon)|)\right), \tag{3.15}$$

$$\left(\frac{\mathrm{d}F}{\mathrm{d}z} + \tfrac{1}{2}F^2\right)\Big|_{z=0} = 2I^{-2/3}\varepsilon^{-2/3}p_1 + z_0, \tag{3.16}$$

$$F(z) = -\frac{1}{z-z_0} \quad \text{for } z \gg z_0 \text{ (QEB)}, \tag{3.17}$$

$$\int_0^z F(z)\,\mathrm{d}z + \ln(z-z_0) + \tfrac{2}{3}\ln\varepsilon - \tfrac{1}{3}\ln I = -V - \Phi(x,t) \quad \text{in QEB}. \tag{3.18}$$

Here parameter z_0 is defined as

$$z_0 = I^{1/3}\varepsilon^{-2/3}y_0.$$

In what follows, we will use this representation of the basic problem for obtaining a unified description of the Q1DL valid for all states of the EDL. Let us recall that (3.17) is a version of the electroneutrality condition following from the assumption of a monotonic increase of F at infinity in (3.15), whereas (3.18) stands for the electric potential drop across the Q1DL. The right-hand side of (3.18) defines the 'reduced' ζ-potential as

$$\zeta(x,t) \stackrel{\text{def}}{=} -V - \Phi(x,t). \tag{3.19}$$

Finally, let us point out that the term on the right-hand side of the boundary condition (3.16), unbounded for $\varepsilon \to 0$ and characteristic of condition (3.2a,b) rewritten in the new variables, implies the presence of a boundary layer near $z = 0$.

Below, for future use, we review various types of solution to the Painleve equation (3.15) and its approximations corresponding to various ranges of parameter $z_0(\varepsilon)$ and, thus, through (3.18), to various ranges of reduced ζ-potential in relation to $\varepsilon \to 0$. The names which we assign to various scenarios associated with these solutions are motivated by the subsequent analysis of transition from quasi-equilibrium to non-equilibrium EDL.

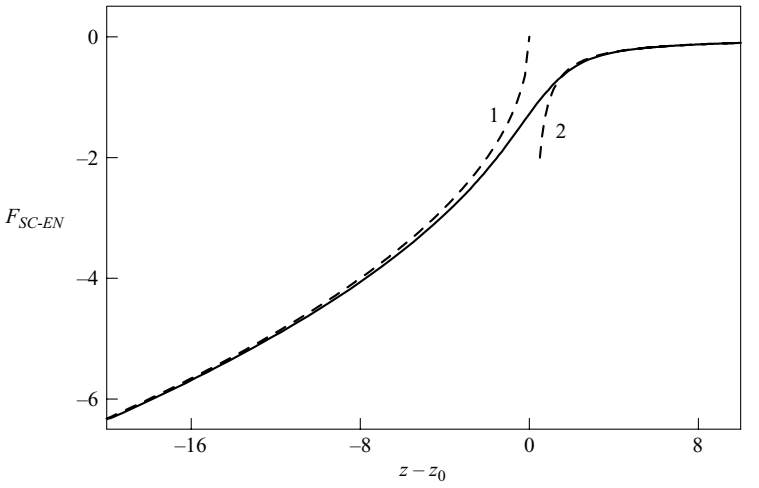

FIGURE 4. Profiles of the transition layer solution $F_{SC\text{-}EN}$ (—), extended space charge region asymptotics $-\sqrt{-2z}$ (- - - 1), and electroneutral asymptotics $-1/z$ (- - - 2).

3.2. *Review of solutions to the basic problem (3.15)–(3.18) for various ranges of parameter z_0 versus ε*

Scenario 1(figure 4). Entire transition layer solution

By looking for a solution of (3.15) on the entire axis $-\infty < z < \infty$ for z_0 fixed (possibly large), we arrive at the transition layer solution

$$F(z) = F_{SC\text{-}EN}(z - z_0) \tag{3.20}$$

connecting between the non-equilibrium space charge region ($z \ll z_0$) and quasi-electroneutral bulk (QEB, $z \gg z_0$). $F_{SC\text{-}EN}(z)$ is the unique Painleve transcendent with the following characteristic asymptotics, inferred from the equation

$$\frac{\mathrm{d}^2 F_{SC\text{-}EN}}{\mathrm{d}z^2} = \tfrac{1}{2} F_{SC\text{-}EN}^3 + z F_{SC\text{-}EN} + 1,$$

by assuming $F_{SC\text{-}EN}$, $F''_{SC\text{-}ENzz}$ vanishing for $z \gg 0$ and $F_{SC\text{-}EN}^3$, $z F_{SC\text{-}EN}$ terms dominating, along with $F_{SC\text{-}ENzz}$ bounded for $z \ll 0$, as

$$F_{SC\text{-}EN}(z) = \begin{cases} -\sqrt{-2z}, & z \ll 0, \\ -\dfrac{1}{z}, & z \gg 0. \end{cases} \tag{3.21a,b}$$

Scenario 2 (Figure 5a,b). Thin quasi-equilibrium EDL (QE–EDL), $z_0 = -O(\varepsilon^{-2/3})$

By assuming $z_0 = -O(\varepsilon^{-2/3}) < 0$ and using the scaling

$$r = z\sqrt{|z_0|}, \quad r_0 = |z_0|\varepsilon^{2/3} \left(= I^{1/3}\,|y_0|\right), \quad R(r) = \frac{F}{\sqrt{|z_0|}}, \tag{3.22a–c}$$

we obtain from (3.15), (3.16), to leading order, the following 'thin QE–EDL' approximation of the Painleve equation

$$\frac{\mathrm{d}^2 R}{\mathrm{d}r^2} = \tfrac{1}{2} R^3 + R \tag{3.23}$$

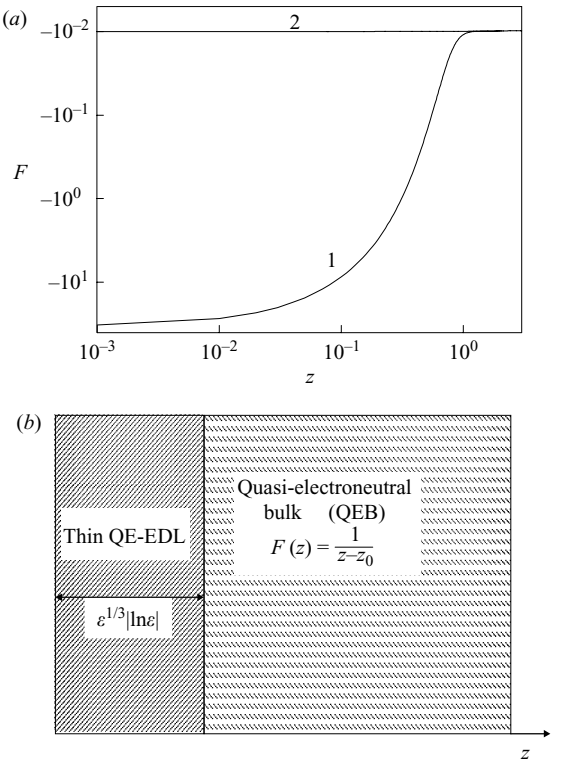

FIGURE 5. Scenario 2. (*a*) Profile of the function $F(z)$ (line 1) and its quasi-electroneutral asymptotics $-1/(z - z_0)$ (line 2). (*b*) Sketch of the structure of Q1DL.

which, considered on the half-axis $0 < r < \infty$, yields, together with boundary condition (3.16) rewritten in terms of R, r as

$$\frac{\mathrm{d}R}{\mathrm{d}r}(0) + \tfrac{1}{2}R^2(0) = 2\frac{p_1}{r_0}I^{-2/3} - 1, \tag{3.24}$$

and the boundedness condition at $r \to \infty$, the exponentially decaying 'Thin QE–EDL' solution of the form

$$R = -2\frac{2\left(2p_1 I^{-2/3}/r_0 - 1\right)\mathrm{e}^{-r}}{\left(\sqrt{2p_1 I^{-2/3}/r_0} + 1\right)^2 - \left(\sqrt{2p_1 I^{-2/3}/r_0} - 1\right)^2 \mathrm{e}^{-2r}}. \tag{3.25}$$

Scenario 3 (figure 6a, b). Thick QE–EDL, $-O(\varepsilon^{-2/3}) < z_0 < -O(1) < 0$

Note that (3.25) remains meaningful for p_0, approaching zero. In this case, R may be viewed as a composition of the following two solutions.

(3a) Inner sublayer of the thick QE–EDL

The first is the algebraically decaying 'thin sublayer' (of the thick QE–EDL) solution of the form

$$Q = -\frac{2}{q + I^{1/3}\sqrt{2/p_1}} \tag{3.26}$$

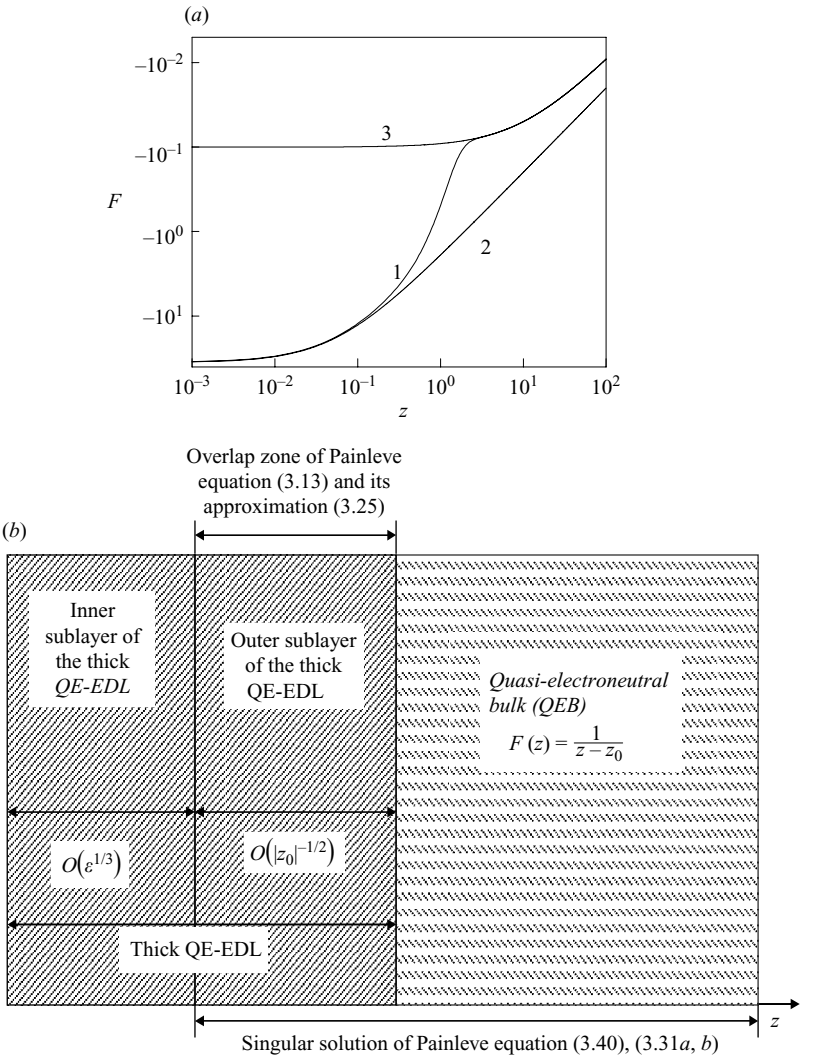

FIGURE 6. Scenario 3. (*a*) Profile of the function $F(z)$ (line 1), its thin QE–EDL asymptotics (3.26), (3.29*a*, *b*) (line 2), and quasi-electroneutral asymptotics $-1/(z - z_0)$ (line 3). (*b*) Sketch of the structure of the Q1DL.

to the following 'inner thin QE–EDL sublayer' approximation to the Painleve equation

$$\frac{\mathrm{d}^2 Q}{\mathrm{d}q^2} = \tfrac{1}{2} Q^3 \tag{3.27}$$

obtained from (3.23) by omitting, to the leading order, the last term, with the similarly obtained from (3.24) boundary condition

$$\frac{\mathrm{d}Q}{\mathrm{d}q}(0) + \tfrac{1}{2} Q^2(0) = 2 p_1 I^{-2/3}. \tag{3.28}$$

Here the following rescaling has been applied

$$q = \frac{z}{\varepsilon^{1/3}} = \frac{r}{\sqrt{|r_0|}}\left(= \frac{y}{I^{1/3}\varepsilon}\right), \quad Q(q) = \varepsilon^{1/3}F = R\sqrt{|r_0|}\left(= I^{-1/3}E\right). \quad (3.29a,b)$$

Let us note that for $q \to \infty$, solution (3.26) behaves as

$$Q^0 \simeq -\frac{2}{q}.$$

Thus, in order to yield (3.25), the inner solution (3.26) is to be matched with the following outer one.

(3b) Outer sublayer of the thick QE–EDL

This is a singular solution to (3.23), satisfying at $r = 0$ the condition

$$R + \frac{2}{r} = O(1).$$

This solution reads

$$R(r) = -4\frac{\mathrm{e}^{-r}}{1-\mathrm{e}^{-2r}}. \quad (3.30)$$

We note that the same solution is recovered from (3.25) by keeping the leading-order terms for $p_0 \ll 1$. Thus, (3.26), (3.29*a*, *b*), (3.30) yield for $-\varepsilon^{-2/3} < O(z_0) < -O(1) < 0$ (y_0 small negative) the following approximation

$$R(r) = -\frac{2}{r + I^{1/3}(2|r_0|/p_1)^{1/2}} + \frac{2}{r} - 4\frac{\mathrm{e}^{-r}}{1-\mathrm{e}^{-2r}} \quad (3.31)$$

to the 'thick QE–EDL' solution (3.25) as a composition of an algebraically decaying solution (3.26) to the approximated Painleve equation (3.27), matched with the exponentially decaying singular solution (3.30) to another approximated version of the Painleve equation (3.23). We will see below that, upon a further increase of z_0 to the 'critical' range $O(1)$, the singular solution (3.30) transforms to that to the full Painleve equation. It will also become evident that singular solutions of this type form an important element of the non-equilibrium EDL in the realistic voltage range. In this sense, 'thick QE–EDL' represents a crucial link between the equilibrium and non-equilibrium EDL.

Scenario 4 (figure 7a, b). Transitional EDL (TEDL), $z_0 = O(1)$

(4a) Inner thin QE sublayer of TEDL

For this range, (3.15) and (3.16) yield, to the leading order on the scale (3.29*a*, *b*), the inner thin QE sublayer problem identical to (3.27) and (3.28) with the algebraically decaying solution (3.26) at infinity.

(4b) Basic singular Painleve solution

Solution (3.26) is to be matched with the basic singular Painleve solution, to the following outer TEDL problem:

$$\frac{\mathrm{d}^2F}{\mathrm{d}z^2} = \tfrac{1}{2}F^3 + (z - z_0)F + 1, \quad (3.32)$$

$$\left(F + \frac{2}{z}\right)\Big|_{z=0} = O(1), \quad F(\infty) = 0. \quad (3.33a,b)$$

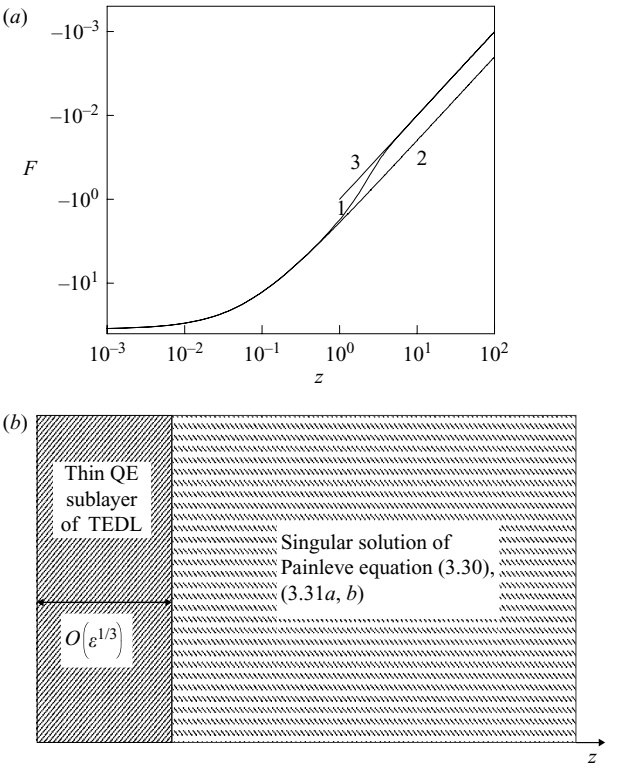

FIGURE 7. Scenario 4. (*a*) Profile of the function $F(z)$ (line 1), its thin QE–EDL asymptotics (3.26), (3.29*a*, *b*) (line 2), and quasi-electroneutral asymptotics $-1/(z-z_0)$ (line 3). (*b*) Sketch of the structure of the Q1DL.

This solution possesses an algebraic singularity at $z=0$ and a 'quasi-electroneutral' asymptotics (3.17) for $z \to \infty$.

Scenario 5 (figure 8a, b). Developed microscopic non-equilibrium space charge regime (mSCR), $O(1) < z_0 < O(\varepsilon^{-2/3})$

(5a) Inner thin QE sublayer for mSCR

For this regime, the scaling (3.29*a*, *b*) yields once more the algebraically decaying solution (3.26).

(5b) Outer thick QE sublayer problem for mSCR

Solution (3.26) is to be matched with a singular solution to the outer thick QE sublayer problem for mSCR,

$$\frac{\mathrm{d}^2 R}{\mathrm{d}r^2} = \tfrac{1}{2}R^3 - R, \quad 0 < r < \infty, \tag{3.34}$$

$$\left(R + \frac{2}{r}\right)\bigg|_{r=0} = O(1), \quad R(\infty) = -\sqrt{2}, \tag{3.35a, b}$$

obtained in a way similar to that which leads to (3.23), (3.24) from (3.15), but, this time, with $|z_0| = z_0$ instead of $|z_0| = -z_0$ in rescaling (3.22*a–c*), in accordance with the positivity of z_0 in the current regime. Note the opposite sign of the last term in (3.34),

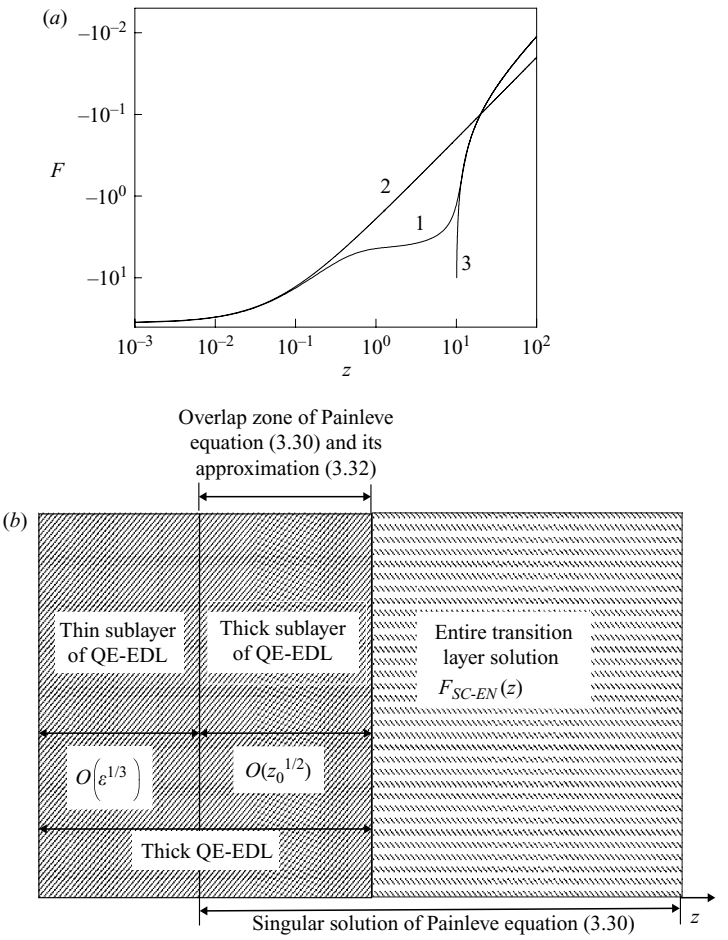

FIGURE 8. Scenario 5. *(a)* Profile of the function $F(z)$ (line 1), its thin QE–EDL asymptotics (3.26), (3.29*a*, *b*) (line 2), and quasi-electroneutral asymptotics $-1/(z-z_0)$ (line 3). *(b)* Sketch of the structure of Q1DL.

compared to that in (3.23), for the same reason. This yields the appearance of a non-zero fixed point on the right-hand side of (3.34) and, correspondingly, the asymptotic condition (3.35*b*) (instead of decay to zero for R in equation (3.30)). Accordingly, the solution to boundary-value problem (3.34), (3.35*a*, *b*) is

$$R = -\sqrt{2}\frac{e^{\sqrt{2}r}+1}{e^{\sqrt{2}r}-1}. \tag{3.36}$$

Note that for $r \to \infty$, this outer thick QE sublayer solution matches exactly with non-equilibrium space charge asymptotics $-\sqrt{2}$ (see (3.21*a*) with $z = -z_0 \ll 0$).

Scenario 6 (figure 9a, b). QE sublayer for macroscopic non-equilibrium space charge regime (MSCR), $0 < z_0 = O(\varepsilon^{-2/3})$

In this case, similarly to (3.23)–(3.25), a regular QE sublayer solution to (3.34) with boundary condition

$$\frac{dR}{dr}(0) + \tfrac{1}{2}R^2(0) = 2\frac{p_1}{r_0}I^{-2/3} + 1,$$

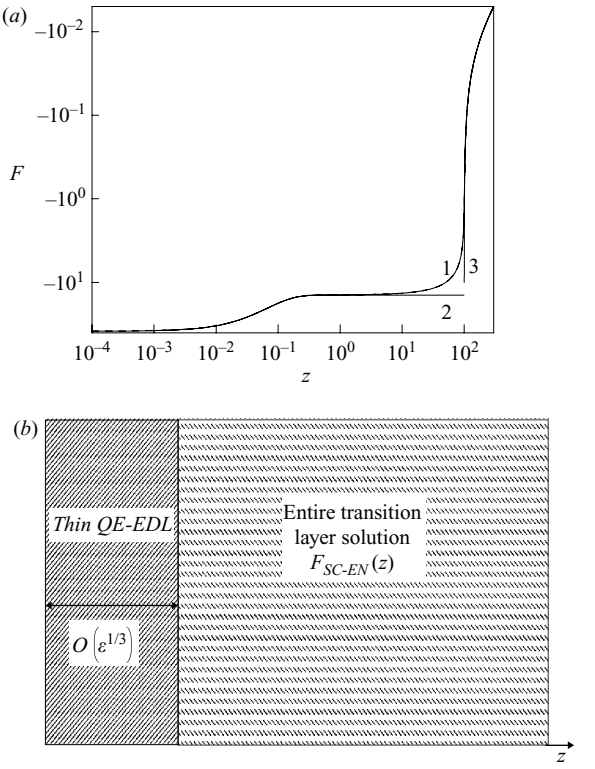

FIGURE 9. Scenario 6. (*a*) Profile of the function $F(z)$ (line 1), its thin QE–EDL asymptotics (3.26, 3.29*a*, *b*) (line 2), and quasi-electroneutral asymptotics $-1/(z-z_0)$ (line 3). (*b*) Sketch of the structure of the Q1DL.

reads in terms of F and z

$$F(z) = -\sqrt{2z_0}\frac{\left(1+\sqrt{\dfrac{p_1}{I^{1/3}y_0}+1}\right)\exp(\sqrt{2z_0}z)+\sqrt{\dfrac{p_1}{I^{1/3}y_0}+1}-1}{\left(1+\sqrt{\dfrac{p_1}{I^{1/3}y_0}+1}\right)\exp(\sqrt{2z_0}z)-\sqrt{\dfrac{p_1}{I^{1/3}y_0}+1}+1}. \tag{3.37}$$

Let us note that, similarly to (3.36), solution (3.37) decays exponentially to the value $-\sqrt{2z_0}$ (instead of zero in (3.25)) and, thus, matches exactly with the extended space charge asymptotics (3.21*a*).

We conclude by recapitulating various notations for the electric field, employed in this and previous section, pertaining to different scalings in different parts of the EDL in various regimes: $E=-\varepsilon\partial\varphi/\partial y$ (3.6), $F=\varepsilon^{1/3}E=-\varepsilon^{2/3}\partial\varphi/\partial y$ (3.14*a*), $R=|z_0|^{-1/2}F$ (3.22*c*), $Q=\varepsilon^{1/3}F$ (3.29*b*).

3.3. *Transition from thin QE–EDL to MSCR upon the increase of V (or $|\zeta|$)*

In this section, we relate each of the scenarios 2–6 to a specific range of ζ, and trace the transition from thin QE–EDL to the MSCR upon the increase of $|\zeta|$. In particular, we will show that the increase of z_0 from $-O(\varepsilon^{-2/3})$ to $O(\varepsilon^{-2/3})$ corresponds to $|\zeta|$ increasing from $O(1)$ to $O(\varepsilon^{-1})$.

Thin QE–EDL $0 = -O(\varepsilon^{-2/3}) < 0 \Rightarrow \zeta(x) = -O(1)$

Let us start with the case of thin QE–EDL near the membrane surface $z = 0$ (scenario 2 of § 3.2). In this case, the Q1DL solution consists of the following two components: thin QE–EDL solution $R(r)$ (3.25) and the following outer QEB solution (compare with (3.17))

$$F_0(z) = -\frac{1}{z - z_0}$$

which match to the leading order $O(\varepsilon^{2/3})$, yielding the following composite solution

$$F_0(z) + \sqrt{|z_0|}R(z\sqrt{|z_0|}) = -\frac{1}{z - z_0} - \frac{4\sqrt{|z_0|}\left(2\dfrac{p_1}{|z_0|\varepsilon^{2/3}}I^{-2/3} - 1\right)\exp(-z\sqrt{|z_0|})}{\left(\sqrt{2\dfrac{p_1}{|z_0|\varepsilon^{2/3}}I^{-2/3}} + 1\right)^2 - \left(\sqrt{2\dfrac{p_1}{|z_0|\varepsilon^{2/3}}I^{-2/3}} - 1\right)^2\exp(-2z\sqrt{|z_0|})}. \quad (3.38)$$

Parameter r_0 (or z_0, or y_0) is related to voltage through integration of (3.25) yielding

$$\int_0^\infty R(r)\,\mathrm{d}r = \zeta_q \overset{\text{def}}{=} -V - \varphi_q(x), \quad (3.39)$$

Here, $\varphi_q(x)$ is the electric potential at the outer edge of thin QE–EDL, and $\zeta_q(x)$ is the quasi-equilibrium portion of the total ζ-potential (the overall potential drop across the Q1DL minus that upon the quasi-electroneutral part of the latter). The latter equality yields

$$r_0 = 2p_1 I^{-2/3}\exp(\zeta_q), \quad (3.40)$$

and

$$y_0 = -\frac{2p_1}{I}\exp(\zeta_q), \quad \zeta_q = \ln\frac{-Iy_0}{2p_1} = O(1). \quad (3.41a,b)$$

By substitution of (3.38) and (3.41*b*) into the overall potential balance (3.18), we obtain

$$\zeta_q + \ln(-y_0) = 2\zeta_q + \ln\left(\frac{2p_1}{I}\right) = \zeta = O(1) \text{ in QEB } \left(\varepsilon < O(y) < \frac{1}{\ln(\varepsilon)}\right). \quad (3.42)$$

Substitution of (3.42) into (3.41*a*) yields

$$y_0 = -\sqrt{\frac{2p_1}{I}}\exp(\zeta/2). \quad (3.43)$$

Thick QE–EDL $0 < O(1) < -O(z_0) < \varepsilon^{-2/3} \Rightarrow \zeta(x) = \alpha|\ln(\varepsilon)| + O(1), 0 < \alpha < 4/3$

We consider next the case of the thick QE–EDL. In this case, the order of magnitude of the control parameter z_0 (or y_0) is

$$z_0 = -O(\varepsilon^{\alpha/2-2/3}), \quad y_0 = -O\left(\varepsilon^{\alpha/2}\right). \quad (3.44a,b)$$

Correspondingly, according to scenario 3 of § 3.2, the composite solution (3.38) is still valid. This solution may be represented this time as the following composition of the algebraically decaying solution (3.25) (which may be viewed as consisting of the

inner sublayer solution (3.26) matched with the exponentially decaying singular outer solution (3.30)) and the quasi-electroneutral solution (3.38):

$$F(z)=\frac{-4\sqrt{|z_0|}\left(2\dfrac{p_1}{|z_0|\varepsilon^{2/3}}I^{-2/3}-1\right)\exp(-z\sqrt{|z_0|})}{\left(\sqrt{2\dfrac{p_1}{|z_0|\varepsilon^{2/3}}I^{-2/3}}+1\right)^2-\left(\sqrt{2\dfrac{p_1}{|z_0|\varepsilon^{2/3}}I^{-2/3}}-1\right)^2\exp(-2z\sqrt{|z_0|})}-\frac{1}{z-z_0} \tag{3.45a}$$

$$F(z)\simeq-\frac{2}{z+I^{1/3}\varepsilon^{1/3}\sqrt{2/p_1}}+\frac{2}{z}-4\sqrt{|z_0|}\frac{\exp(-\sqrt{|z_0|}z)}{1-\exp(-2\sqrt{|z_0|}z)}-\frac{1}{z-z_0}. \tag{3.45b}$$

By evaluating the potential drop across thick QE–EDL through integration of (3.25) as we did previously in (3.39)–(3.41a, b), (3.42), (3.43), we find that

$$y_0=-\frac{2p_1}{I}\exp(\zeta_q)\simeq-\sqrt{\frac{2p_1}{I}}\exp(\zeta/2), \tag{3.46}$$

which is still identical to (3.41a).

We note that both the thick QE–EDL solution (3.45a) and its approximation (3.45b) yield the same expression for y_0. Indeed, by substituting (3.45b) (without the QEB component $-1/(z-z_0)$ into (3.39) for the overall potential drop across QE–EDL, we obtain

$$\int_0^\infty\left(-\frac{2}{z+I^{1/3}\varepsilon^{1/3}\sqrt{2/p_1}}+\frac{2}{z}-4\sqrt{|z_0|}\frac{\exp(-z\sqrt{|z_0|})}{1-\exp(-2z\sqrt{|z_0|})}\right)\mathrm{d}z=\zeta_q. \tag{3.47}$$

By integration in the left-hand side of (3.47), we recover (3.46) for the parameter y_0. Thus, although the approximate formula (3.45b) is not valid point-wise for $\zeta=-O(1)$, it still provides the exact expression for y_0 for all values of ζ-potential in the range $O(1)\leqslant|\zeta|<O\left(4|\ln\varepsilon|/3\right)$. We explain this 'paradox' in Appendix A.

Critical case: $z_0=O(1)\Rightarrow\zeta=O(4/3\ln\varepsilon)$. Transition from thick QE–EDL to NE–EDL via TEDL

Let us consider the critical case

$$y_0=O\left(\varepsilon^{2/3}\right),\quad z_0=O(1).$$

In this case, the Q1DL solution is essentially that for TEDL described by scenario 4. Let us recall that in this case, the thick QE–EDL transforms into the non-equilibrium EDL occupying the layer $0<z\leqslant O(1)$ with the overall Q1DL solution consisting of the following two components: algebraically decaying thin QE–EDL solution (3.26) matched with the singular Painleve solution (3.32), (3.33a, b). Thus, the leading-order term of the overall composite solution reads

$$F_{(0)}(z)=-\frac{2}{z+\varepsilon^{1/3}I^{1/3}\sqrt{2/p_1}}+F(z)+\frac{2}{z}. \tag{3.48}$$

Here $F(z)$ is the singular Painleve solution (3.32), (3.33a, b). In Appendix B, we show that the contribution of higher-order corrections into this composite solution is of

the order of $O(\varepsilon^{1/3})$. This yields to the leading order for the reduced ζ-potential:

$$\int_0^z \left(\frac{2}{z} - \frac{2}{z + \varepsilon^{1/3} I^{1/3} \sqrt{2/p_1}} + F(z) \right) \mathrm{d}z + \tfrac{2}{3} \ln \varepsilon - \tfrac{1}{3} \ln I + \ln(z - z_0) + O\left(\varepsilon^{1/3}\right) = \zeta, \tag{3.49}$$

where $z \in \mathrm{Q1DL} \cap \mathrm{QEB}$.

In order to simplify (3.49), let us define the regular part $G(z)$ of the singular Painleve solution as

$$G(z) = F(z) + \frac{2}{z}. \tag{3.50}$$

Substitution of (3.50) into problem (3.32), (3.33a, b) yields the following boundary-value problem for $G(z)$

$$\frac{\mathrm{d}^2 G}{\mathrm{d}z^2} = \tfrac{1}{2} G^3 + \frac{6}{z^2} G - \frac{3}{z} G^2 + zG - 1 + z_0 \left(\frac{2}{z} - G \right) \quad (0 < z < \infty), \tag{3.51}$$

$$G(0) = O(1), \quad G(z) = \frac{2}{z} - \frac{1}{z - z_0} \text{ for } z - z_0 \gg 1. \tag{3.52a, b}$$

For small z, the requirement of boundedness of $G(z)$ at $z = 0$ yields the expansion

$$G(z) = -\frac{z_0}{3} z + \tfrac{1}{4} z^2 + \cdots \tag{3.53}$$

Let us point out that function G is controlled by a single parameter z_0. In terms of $G(z)$, (3.49) reads

$$P(z_0) + \tfrac{4}{3} \ln \varepsilon + \ln \frac{2}{p_1} + \tfrac{1}{3} \ln I = \zeta. \tag{3.54}$$

Here,

$$P(z_0) \stackrel{\text{def}}{=} \int_0^\infty \left(G(z) - \frac{1}{z + 1} \right) \mathrm{d}q. \tag{3.55}$$

In figure 10, we present the z_0 versus ζ curve calculated from (3.54), (3.55) for $I = 2$, $p_1 = 10$ and $\varepsilon = 10^{-5}$.

We observe from this curve that z_0 unboundedly decreases to $-\infty$ as $\zeta \to 0$, and so does the last term on the right-hand side of (3.51), thus, generating a $(1/\sqrt{|z_0|})$-thick boundary layer near $z = 0$. For this boundary layer, through rescaling (3.22a–c) we immediately recover the thick QE–EDL (scenario 3) solution $R(r)$, (3.31), as the low reduced ζ-potential asymptotics of the TEDL solution (3.48). We point out that z_0 found as a solution to (3.54) matches remarkably well with the value predicted by (3.41a), (3.46) derived for very different conditions. To illustrate this statement, let us extrapolate (3.42), determining the quasi-equilibrium portion ζ_q of ζ and valid for $O(1) \leqslant |\zeta| < 4/3 |\ln \varepsilon|$, to the critical case $|\zeta| = O(4/3 |\ln \varepsilon|)$ and compare z_0 calculated from (3.54), (3.55) (line 1 in figure 10) with that obtained from (3.41a), (3.46) (line 2 in figure 10). Based on the extremely close agreement between $\zeta \ll -1$ asymptotics of z_0 calculated from (3.54) and z_0 obtained from (3.46), we conclude that (3.54) derived for the 'critical' range $\zeta = O(4/3 \ln \varepsilon)$ yields a correct value of parameter z_0 (and, thus, also of y_0) for the entire range of ζ from quasi-equilibrium ($\zeta = -O(1)$) to $\zeta = O(4/3 \ln \varepsilon)$.

To complete the discussion of the critical case $z_0 = O(1)$, we observe that (3.54) directly yields the estimate $\zeta = O(4/3 \ln \varepsilon)$.

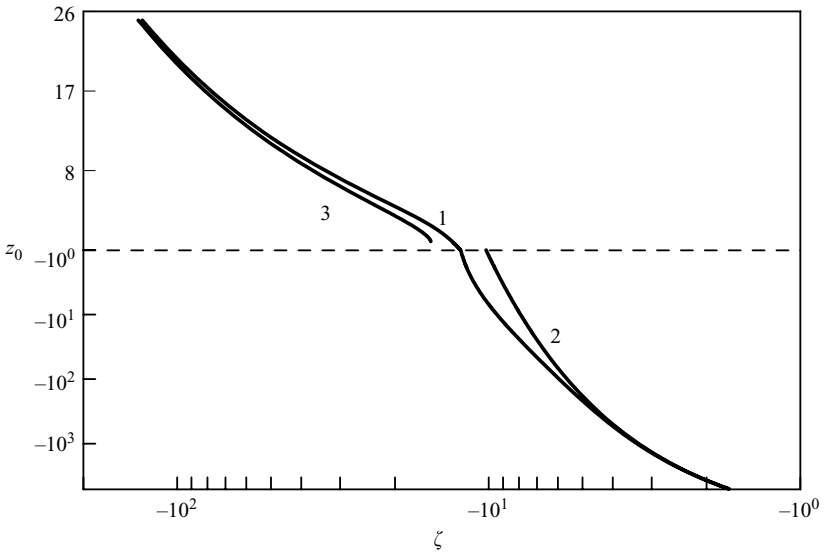

FIGURE 10. Profile of z_0 as a function of ζ (line 1), and quasi-equilibrium (line 2) and developed non-equilibrium space charge regime (line 3) asymptotics of z_0.

Developed microscopic non-equilibrium space charge zone
$O(1) < z_0 < O(\varepsilon^{-2/3}) \Rightarrow |4/3 \ln \varepsilon| < O(|\zeta|) < O(1/\varepsilon)$

Let us finish this section with the analysis of the two regimes of developed non-equilibrium space charge produced by overcritical reduced ζ-potentials. We begin with the microscopic non-equilibrium space charge case occurring for ζ in the range $|4/3 \ln \varepsilon| < O(|\zeta|) < O(1/\varepsilon)$. According to scenario 5, in this cases, the Q1DL solution consists of the following three components:

(i) Algebraically decaying thin QE–EDL solution (3.26), matched with

(ii) Thick QE–EDL solution (3.34), (3.35a, b) exponentially decaying to $-\sqrt{2z_0}$. This latter value corresponds to

(iii) Non-equilibrium space-charge asymptotics $-\sqrt{2z_0}$ ((3.21a) with $z = -z_0 \ll 0$). The solution of (3.15) for such large values of parameter z_0 is approximated well by the entire transition layer solution (3.20).

Summarizing, the leading-order composite solution for the mSCR reads

$$F(z) = -\frac{2}{z + I^{1/3}\varepsilon^{1/3}\sqrt{2/p_1}} + \frac{2}{z} - \sqrt{2z_0}\frac{\exp(\sqrt{2z_0}z) + 1}{\exp(\sqrt{2z_0}z) - 1} + F_{SC\text{-}EN}(z - z_0) + \sqrt{2z_0}. \quad (3.56)$$

Substitution of (3.56) into (3.18) yields

$$2\sqrt{2Iz_0^3}/3 = -\left(\zeta - \tfrac{4}{3}\ln\varepsilon - \tfrac{1}{3}\ln I\right) + O(1), \quad (3.57)$$

and, thus,

$$z_0 = \frac{3^{2/3}}{2I^{1/3}}\left|\zeta - \tfrac{4}{3}\ln\varepsilon - \tfrac{1}{3}\ln I\right|^{2/3} + O(1). \quad (3.58)$$

Equation (3.58) implies that whenever the following inequality holds

$$z_0\varepsilon^{2/3} \ll \frac{1}{|\ln\varepsilon|}, \quad (3.59)$$

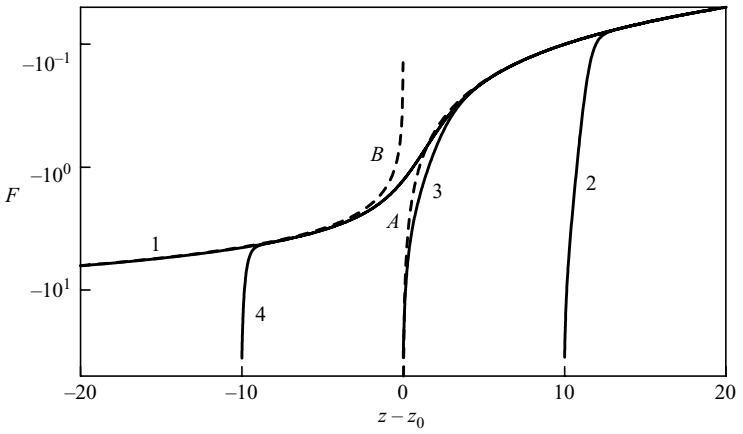

FIGURE 11. Profile of F as a function of $z-z_0$: 1, entire transition layer solution $F_{SC\text{-}EN}$; 2, scenario 3, $z_0=-10$; 3, scenario 4, $z_0=0$; 4, scenario 5, $z_0=10$; A, quasi-electroneutral asymptotics $-1/(z-z_0)$; B, non-equilibrium space charge asymptotics $-\sqrt{-2(z-z_0)}$.

we have

$$\zeta \geqslant -O\left(\frac{1}{\varepsilon|\ln\varepsilon|^{3/2}}\right) > -O\left(\frac{1}{\varepsilon}\right). \tag{3.60}$$

Inequality (3.60) yields an upper bound estimate for applicability of quasi-one-dimensional analysis. We reiterate that (3.58) follows from (3.54), (3.56) and asymptotic expansion (3.21a) for $z_0 \to \infty$.

In figure 10, we compare once more z_0 obtained from (3.54), for $\zeta = O(4/3\ln\varepsilon)$ (line 1), with that obtained from (3.58) for $|4/3\ln\varepsilon| < O(|\zeta|)$ (line 3). Based on this comparison, we broaden our previous conclusion concerning the range of validity of (3.54). In fact, this equation, together with (3.49), (3.54) yields a correct value of parameter z_0 (and, thus, also of y_0) for the entire range of reduced ζ-potential from quasi-equilibrium ($\zeta(x)=O(1)$) to the mSCR $|4/3\ln\varepsilon| < O(|\zeta|) < O(1/\varepsilon)$.

Macroscopic non-equilibrium space charge regime $0 < z_0 = O(\varepsilon^{-2/3}) \Rightarrow |\zeta| \geqslant O(1/\varepsilon)$

For still larger reduced ζ-potentials ($|\zeta| \geqslant O(1/\varepsilon)$), the width of the non-equilibrium space charge zone exceeds $O(1/|\ln\varepsilon|)$ and may reach $O(1)$, thus, violating the assumed one-dimensionality. In this case, the above analysis is still applicable for strictly one-dimensional electrodiffusional situations. For scenario 7, the one-dimensional electrodiffusional solution is the following composition of the entire transition layer solution and thin QE–EDL solution:

$$F(z) = 2\sqrt{2z_0}\,\frac{1-\sqrt{\dfrac{p_1}{I^{1/3}y_0}+1}}{\left(1+\sqrt{\dfrac{p_1}{I^{1/3}y_0}+1}\right)\exp(\sqrt{2z_0}z)+1-\sqrt{\dfrac{p_1}{I^{1/3}y_0}+1}} + F_{SC\text{-}EN}(z-z_0). \tag{3.61}$$

By keeping the leading-order terms in (3.58), we obtain

$$z_0 = \frac{3^{2/3}}{2I^{1/3}}|\zeta|^{2/3}.$$

Figure 11 gives a summary of the asymptotic solutions of this section superimposed upon the entire transition layer solution $F_{SC\text{-}EN}$ (3.20), but, the discussion of charge distribution in the EDL for different ranges of ζ (or z_0) is deferred to Appendix B.

3.4. *Limiting two-dimensional QEB electrodiffusion problem*

We are set now to formulate the full limiting two-dimensional electrodiffusion problem in the quasi-electroneutral bulk (QEB) for the regimes with 'thin charged layers' (scenarios 2–5, $O(1) \leqslant -\zeta < O(1/\varepsilon)$). This problem will consist of the following two subproblems: that for the QEB proper, to be solved in the domain $\{-\infty < x < \infty, 0 < y < 1\}$, and that for the Q1DL. The latter has been analysed above, yielding the crucial parameter $y_0(x,t)$. Recall that according to (3.8), y_0 is the extrapolated position at which the QEB concentration vanishes. The Q1DL analysis provides, through (3.54), y_0 as a function of the data of the quasi-one-dimensional problem which are the boundary values of regular parts of the solutions to the QEB problem ($\Phi(x,t) = \phi(x,0,t)$ and $I(x,t) = i(x,0,t)$). We begin with formulation of the leading order ($\varepsilon = 0,\ O(|\ln\varepsilon|) = \infty$) QEB problem:

3.4.1. *Leading-order singular QEB problem*

For the relevant range of ζ, y_0 lies in the range $-O(1) \leqslant y_0 \leqslant O(\varepsilon^{2/3})$. Thus, in accordance with (3.8), the crucial boundary condition for concentration at the depleted boundary $y = 0$ is, to the leading order,

$$\overline{c}(x,0,t) = \begin{cases} -y_0 \dfrac{\partial \overline{c}}{\partial y}(x,0,t) & (y_0 \leqslant 0), \\ 0 & (y_0 \geqslant 0). \end{cases} \tag{3.62}$$

We note that, according to the above Q1DL analysis (3.41*a*), (3.46), for $O(y_0) < -\varepsilon^{2/3}$, condition, (3.62) is the standard local equilibrium condition, implying continuity of electrochemical potential of counter-ions at the membrane/solution interface. (This ceases to be the case in the critical regime, for $O(y_0) = -\varepsilon^{2/3}$.)

The rest of the QEB formulation is straightforward. It comprises the impermeability condition for co-ions at $y = 0$

$$\frac{\partial \overline{c}}{\partial y} - \overline{c}\frac{\partial \overline{\varphi}}{\partial y} = 0; \tag{3.63}$$

and the standard local equilibrium and co-ions impermeability conditions at the 'enriched' boundary $y = 1$:

$$(\ln \overline{c} + \overline{\varphi})\,|_{y=1} = \ln p_1, \qquad \left(\frac{\partial \overline{c}}{\partial y} - \overline{c}\frac{\partial \overline{\varphi}}{\partial y}\right)\bigg|_{y=1} = 0; \tag{3.64a,b}$$

and the equations of quasi-electroneutral electrodiffusion for the ionic concentration and electric potential:

$$\frac{\partial \overline{c}}{\partial t} = \Delta \overline{c}, \quad \nabla \cdot \left(\frac{1-D}{1+D}\nabla \overline{c} - \overline{c}\nabla \overline{\varphi}\right) = 0,\ |x| < \infty,\ 0 < y < 1,\ t > 0. \tag{3.65a,b}$$

The boundary values of the regular potential $\Phi(x,t) = \ln(I(x,t)/2) - \mu^-(x,0,t)$ and the electric current density $i(x,0,t) = 2\partial c/\partial y(x,0,t) = I(x,t)$ provide the data for (3.54) for y_0.

For vanishing boundary concentration, the problem (3.62)–(3.65a,b) is an instance of those with a boundary degeneracy in the elliptic equation (3.65b). (A common example of such problems is the extensively studied porous medium equation; see Kamin, Peletier & Vazquez 1989).

Restricting ourselves to consideration of strong depletion $|y_0| \ll 1$ at $y = 0$, we may simplify the formulation of the outer problem (3.62)–(3.65a,b). In this case, the

boundary condition (3.62) may be rewritten as

$$\overline{c}(x,0,t)=0.$$

Let us note that, to the leading order considered here, electrochemical potential of cations $\ln\overline{c}+\overline{\varphi}$ is infinite at the depleted boundary $y=0$ for $y_0\geqslant 0$ and, accordingly, the vanishing concentration at the depleted boundary corresponds to an infinite voltage V. Formulation (3.62)–(3.65a,b) is not very useful because it yields short-wave singularity in electro-osmotic instability which constitutes the main topic of our concern (see Rubinstein & Zaltzman 2003; Rubinstein *et al.* 2005). Thus, these formulations require regularization which may be achieved by accounting for the next-order terms in the cationic electrochemical potential. This yields the following regular formulation.

3.4.2. *Regular QEB problem*

We regularize limiting formulation (3.62)–(3.65a,b) by taking into account the leading-order correction to the boundary value of the QEB cationic electrochemical potential, which is of the order $O(1)$ for quasi-equilibrium and $O(|\ln\varepsilon|)$ for non-equilibrium regimes. We also note that, for all regimes, the anionic electrochemical potential is constant in the Q1DL and is equal to

$$\mu^-=\ln c^- -\varphi=\ln\frac{I}{2}-\Phi(x,t),\quad y\in \mathrm{Q1DL}\cap\mathrm{QEB}.$$

Equations (3.8), (3.11) yield

$$\mu^+=\ln\frac{I}{2}+\Phi(x,t)+2\ln(y-y_0)\ \text{in Q1DL}\cap\mathrm{QEB}. \tag{3.66}$$

Let us take $y=y_1$ in (3.66), where y_1 is the outer edge of the EDL. Then, for the quasi-equilibrium EDL ($O(|\zeta|)=\alpha|\ln\varepsilon|$, $0<\alpha<4/3$), (3.44a,b) yield

$$O(\varepsilon^{1/3-\alpha/4})=O(|z_0|^{-1/2}\varepsilon^{2/3})\ll y_1\ll -y_0=O(\varepsilon^{-\alpha/2}),$$

and, thus, substitution of (3.43), (3.46) into (3.66) yields

$$\mu^+=\ \ln p_1-V,\quad \text{for } O(|\zeta|)<\tfrac{4}{3}|\ln\varepsilon|. \tag{3.67}$$

For $O(|\zeta|)\geqslant\frac{4}{3}|\ln\varepsilon|$, (3.19), (3.54), (3.55) and (3.66) yield for $z\in$ Q1DL$\cap$QEB

$$\mu^+=\ln\frac{p_1(z-z_0)^2}{4}-V-P(z_0). \tag{3.68}$$

Substituting asymptotic relations (3.56), (3.57) into (3.50), (3.55) and, keeping leading-order terms, we find from (3.54) for $z_0\geqslant O(1)$, ($4/3|\ln\varepsilon|\leqslant O(|\zeta|)$):

$$P(z_0)=O(1)+\frac{(2\max(z_0,0))^{3/2}I^{1/2}}{3}. \tag{3.69}$$

Equations (3.68), (3.69) applied at the outer boundary of the Q1DL z_1, yield the sought generalization for non-equilibrium regimes of continuity condition (3.67). The question is where to place z_1? Clearly, it has to be to the right of the outer edge of the EDL. We argue that, with a reasonable choice of z_1, for all our relevant non-equilibrium regimes $4/3|\ln\varepsilon|\leqslant O(|\zeta|)<1/\varepsilon$, the difference z_1-z_0 is independent

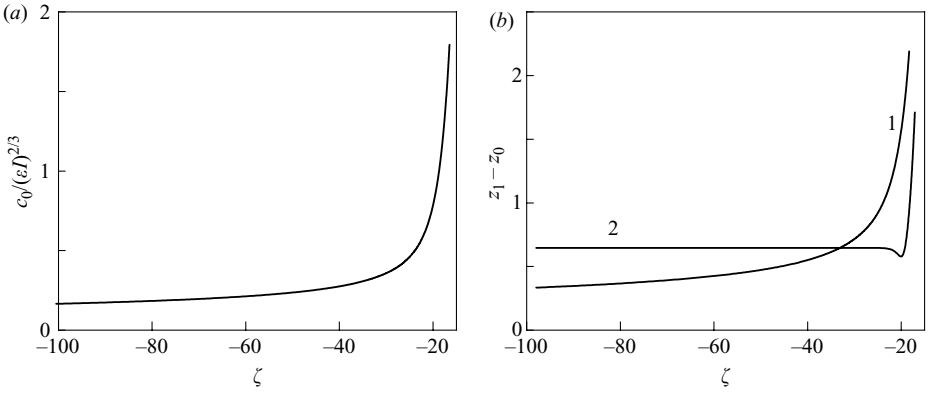

FIGURE 12. Minimum cationic concentration c_0 (*a*) and relative position of the outer edge of EDL $z_1 - z_0$ (*b*): (1, according to Definition 1; 2, according to Definition 2) as functions of ζ for $\varepsilon = 10^{-5}$.

of ζ and ε, that is

$$\ln(z_1 - z_0) = O(1). \tag{3.70}$$

To illustrate this, let us compare the following two definitions of z_1.

Definition 1. Let us use a stepwise approximation for the cationic concentration profile, of the kind employed by Nikonenko *et al.* (1989) by assuming

$$\overline{c} = c_0 \overset{\text{def}}{=} \min c^+_{EDL}$$

in the EDL outside the quasi-equilibrium sublayer up to the cross-section with the linear QEB solution, and let us identify z_1 with the position of the cross-section point. This yields

$$z_1 = \frac{2c_0}{(\varepsilon I)^{2/3}} + z_0. \tag{3.71}$$

In figure 12(*a*), we present the c_0 versus ζ curve calculated from (3.7), (3.14*a*), (3.15)–(3.18). The dependence of z_1 on ζ is presented in figure 12(*b*) (curve 1). Then, using (3.71) we find that

$$\ln(z_1 - z_0) = \ln\frac{c_0}{\varepsilon^{2/3}} - \ln\frac{2}{I^{2/3}} = O(1)$$

for $4/3|\ln\varepsilon| \leqslant O(|\zeta|) < 1/\varepsilon$.

Definition 2. Let us define the relative space charge density as

$$\rho \overset{\text{def}}{=} \frac{c^+ - c^-}{c^+}.$$

ρ monotonically decreases in the Q1DL from 1 to 0, and, accordingly, its derivative $\partial\rho/\partial y$ is negative and almost vanishes at $y = 0$, where c^- is negligibly small and $\rho \simeq 1$, and in QEB, where $\rho \simeq 0$. Thus, let us identify y_1 with the point of minimum of $\partial\rho/\partial y$ that is with the inflection point of $\rho(y)$:

$$\frac{\partial^2\rho}{\partial y^2}(y_1) = 0. \tag{3.72}$$

In figure 12(*b*) (curve 2), we plot the dependence of thus defined $z_1 = \varepsilon^{-2/3} I^{1/3} y_1$ on ζ. We note the proximity of curves 1, 2 in figure 12(*b*) for $|\zeta| \gg 1$. We also point out

that the difference $z_1 - z_0$ in curve 2 converges to the value 0.66 for still larger values of $-\zeta$. This limit corresponds to the solution of (3.72) with relative space charge density taken from the entire transition layer solution (3.20).

Obviously, these two definitions are purely heuristic, and serve only for illustration of the approximate (by the order of magnitude) independence of the difference $z_1 - z_0$ of ε, ζ for non-equilibrium regimes.

Summarizing, (3.67)–(3.70) yield

$$\mu^+ = \ln p_1 - V\left[1 + O\left(\frac{1}{|\ln\varepsilon|}\right)\right] - \frac{(2\max(z_0,0))^{3/2} I^{1/2}}{3}, \tag{3.73}$$

for the entire range of ζ from quasi-equilibrium ($\zeta = O(1)$) to the developed non-equilibrium space charge regime $|4/3 \ln\varepsilon| < O(|\zeta|) < O(1/\varepsilon)$. Equation (3.73) is a generalization for non-equilibrium conditions of the common continuity of electrochemical potential of counter-ions. Note that for quasi-equilibrium ($z_0 < 0$) it is reduced to the usual continuity condition (3.67), whereas for the non-equilibrium regime ($z_0 > 0$) the last term in (3.73) is the leading-order correction to the interface value of the counter-ion electrochemical potential.

For completeness, we reproduce the entire regular formulation of the QEB electrodiffusion problem:

$$\frac{\partial \overline{c}}{\partial t} = \Delta \overline{c}, \quad \nabla \cdot \left(\frac{1-D}{1+D}\nabla \overline{c} - \overline{c}\nabla\overline{\varphi}\right) = 0, \ |x| < \infty, \ 0 < y < 1, \ t > 0; \tag{3.74a,b}$$

$$\ln \overline{c} + \overline{\varphi}(x,0,t) = \ln p_1 - V - (2\max(z_0,0))^{3/2} I^{1/2}/3, \tag{3.75}$$

$$\frac{\partial \overline{c}}{\partial y}(x,0,t) - \overline{c}(x,0,t)\frac{\partial \overline{\varphi}}{\partial y}(x,0,t) = 0; \tag{3.76}$$

$$\ln \overline{c}(x,1,t) + \overline{\varphi}(x,1,t) = \ln p_1, \tag{3.77}$$

$$\frac{\partial \overline{c}}{\partial y}(x,1,t) - \overline{c}(x,1,t)\frac{\partial \overline{\varphi}}{\partial y}(x,1,t) = 0; \tag{3.78}$$

where z_0 is a solution of (3.54) with

$$I(x,t) = 2\frac{\partial \overline{c}}{\partial y}(x,0,t), \tag{3.79}$$

$$\Phi(x,t) = \varphi(x,0,t) - \ln \overline{c}(x,0,t) + \ln \frac{\partial \overline{c}}{\partial y}(x,0,t) = \ln \frac{I(x,t)}{2} - \mu^-(x,0,t). \tag{3.80}$$

Let us note that for $z_0 > O(1)$, substitution of (3.58), (3.80) into boundary condition (3.75) yields to the leading order

$$\ln \overline{c}(x,0,t) + \overline{\varphi}(x,0,t) \simeq \Phi + \tfrac{4}{3}\ln\varepsilon - \tfrac{1}{3}\ln I,$$

and

$$\overline{c}(x,0,t) \simeq \left(\varepsilon \frac{\partial \overline{c}}{\partial y}(x,0,t)\right)^{2/3}, \tag{3.81}$$

previously obtained heuristically in Rubinstein & Zaltzman (2003).

4. Transition from quasi-equilibrium to non-equilibrium electro-osmotic slip

Reuss (1809) was the first to describe the motion of an electrolyte along a charged surface under the influence of an applied electric field (electro-osmosis). Helmholtz

(1879) and Smoluchowski (1914) provided its first explanation nearly a century later, based on a heuristic analysis of the EDL valid for solids impermeable to ions. A systematic theory of quasi-equilibrium electro-osmosis at charge selective solids was finalized in the early 1970s by Dukhin (see Dukhin & Derjaguin 1976). Below we employ our unified picture of the EDL undercurrent to develop such a theory, universally valid for all regimes.

The current section is organized as follows. We begin by deriving for the range $|z_0| < O(\varepsilon^{-2/3}/\ln(\varepsilon))$ a universal electro-osmotic slip condition valid for all realistic regimes except for that corresponding to the thin QE–EDL ($V = O(1)$). We show next that for a thick QE–EDL this condition is reduced to the limiting quasi-equilibrium one:

$$u(x, 0, t) = 2 \ln 2 \frac{\partial \mu^-}{\partial x}(x, 0, t).$$

Finally, we match the obtained universal condition with the sublimiting quasi-equilibrium one of the form

$$u(x, 0, t) = -2 \frac{\partial \mu^-}{\partial x}(x, 0, t) \ln \frac{1 + e^{\zeta_q}}{2}, \tag{4.1}$$

and explore the asymptotic limit of electro-osmotic slip in the regime of developed non-equilibrium space charge $z_0 > O(1)$.

Let us start with the analysis of

4.1. *Contribution of Q1DL ∩ QEB to slip velocity*

To find the tangential velocity, we have to solve the following 'inner' problem

$$-\frac{1}{2}\frac{\partial}{\partial x}\left[\left(\frac{\partial \varphi}{\partial y}\right)^2\right] + \frac{\partial \varphi}{\partial x}\frac{\partial^2 \varphi}{\partial y^2} + \frac{\partial^2 u}{\partial y^2} = 0, \quad u|_{y=0} = 0, \tag{4.2a,b}$$

and match its solution with the respective QEB solution. By substituting the Q1DL ∩ QEB asymptotics (3.11*a*) into (4.2), we obtain

$$\frac{\partial^2}{\partial y^2}\left[u(x, y, t) + \varphi(x, y, t)\frac{\partial \Phi}{\partial x}(x, t)\right] = 0 \text{ in Q1DL} \cap \text{QEB}. \tag{4.3}$$

Equation (4.3) implies that in Q1DL ∩ QEB, the derivative $\partial\left[u + \varphi \partial \Phi/\partial x\right]/\partial y$ is to the leading order a constant, which we shall denote as $\widetilde{U}$. Thus,

$$\frac{\partial}{\partial y}\left[u + \varphi \frac{\partial \Phi}{\partial x}\right] = U' \text{ in Q1DL} \cap \text{QEB}. \tag{4.4}$$

The constant U' is provided by the solution of the QEB problem and is of the order $O(1)$ for a thin QE–EDL and of a larger order otherwise.

Let us rewrite the inner problem (4.2*a*, *b*), (4.4) in terms of 'reduced' velocity $U(x, y, t)$ defined as

$$U(x, y, t) \stackrel{\text{def}}{=} u + [\varphi + V]\frac{\partial \Phi}{\partial x} - yU'. \tag{4.5}$$

Substitution of (4.5) into (4.2*a*, *b*) yields

$$-\frac{1}{2}\frac{\partial}{\partial x}\left[\left(\frac{\partial \varphi}{\partial y}\right)^2\right] + \left(\frac{\partial \varphi}{\partial x} - \frac{\partial \Phi}{\partial x}\right)\frac{\partial^2 \varphi}{\partial y^2} + \frac{\partial^2 U}{\partial y^2} = 0, \tag{4.6}$$

$$U|_{y=0} = 0, \quad \frac{\partial U}{\partial y} = 0 \text{ in Q1DL} \cap \text{QEB}. \tag{4.7a,b}$$

We note that U is constant in Q1DL$\cap$QEB. Thus, the reduced velocity is that part of the total slip velocity which develops entirely in the EDL, without the contribution of the 'bulk' electroconvective velocity developing in Q1DL$\cap$QEB and equal to $yU' - [\varphi + V]\partial\Phi/\partial x$.

It will be shown in due course (see (4.32)) that this latter contribution is universally present everywhere, including the EDL, and results in the classical Helmholtz–Smoluchowski component to the slip velocity (which may be occasionally compensated by some other contributions, such as tangential pressure variations in the EDL).

4.2. *Contribution of EDL to slip velocity*

Let us formulate the boundary-value problem for U in terms of the inner variable z. From (3.6), (3.14a), (3.48), (3.50), we have in terms of the inner variables $z = yI^{1/3}\varepsilon^{-2/3}$, $z_0 = y_0 I^{1/3}\varepsilon^{-2/3}$ for $O(\zeta) < -1$:

$$\varphi = -V + 2\left[\ln\left(y + \varepsilon\sqrt{\frac{2}{p_1}}\right) - \ln\left(\varepsilon\sqrt{\frac{2}{p_1}}\right)\right] - \int_0^z G(s, z_0)\,\mathrm{d}s, \tag{4.8}$$

$$\varphi_x = -\frac{1}{3I}\frac{\partial I}{\partial x} z G - \frac{\partial z_0}{\partial x}\int_0^z \frac{\partial G}{\partial z_0}(s, z_0)\,\mathrm{d}s, \tag{4.9}$$

$$\frac{\partial^2\varphi}{\partial x\partial y} = -\frac{G(z, z_0)}{3I^{2/3}\varepsilon^{2/3}}\frac{\partial I}{\partial x} - \frac{I^{1/3}}{\varepsilon^{2/3}}\frac{\partial G}{\partial z_0}\frac{\partial z_0}{\partial x} - \frac{z}{3I}\frac{\partial G}{\partial z}\frac{\partial I}{\partial x}, \tag{4.10}$$

$$\frac{\partial^2\varphi}{\partial y^2} = -\frac{2}{\varepsilon^{4/3}\left(z + \varepsilon^{1/3}\sqrt{2/p_1}\right)^2} - \frac{I^{2/3}}{\varepsilon^{4/3}}\frac{\partial G}{\partial z}, \tag{4.11}$$

and, using (3.19), (3.54), (3.55), we conclude that

$$\frac{\partial\Phi}{\partial x} = -\frac{1}{3I}\frac{\partial I}{\partial x} - \frac{\partial z_0}{\partial x}\int_0^z \frac{\partial G}{\partial z_0}, \tag{4.12}$$

where $G(z, z_0)$ is defined by (3.50).

Substitution of (4.8)–(4.11) into (4.6), (4.7) yields for U the following boundary-value problem, $z > 0$:

$$\begin{aligned}\frac{\partial^2 U}{\partial z^2} = {} & \frac{1}{3I}\frac{\partial I}{\partial x}\left(G^2 - \frac{2G}{z + A} - \frac{2z}{z + A}\frac{\partial G}{\partial z} - \frac{2z}{(z + A)^2}G\right) \\ & + \frac{\partial z_0}{\partial x}\left(\frac{\partial G}{\partial z_0}\left[G - \frac{2}{z + A}\right] + \int_0^z \frac{\partial G}{\partial z_0}dz\left[\frac{\partial G}{\partial z} + \frac{2}{(z + A)^2}\right]\right) \\ & - \frac{\partial\Phi}{\partial x}\left(\frac{\partial G}{\partial z} + \frac{2}{(z + A)^2}\right);\end{aligned} \tag{4.13}$$

$$U|_{z=0} = 0, \qquad \frac{\partial U}{\partial z} \to 0 \qquad \text{for} \qquad z - z_0 \gg 1, \tag{4.14a, b}$$

where

$$A = \varepsilon^{1/3} I^{1/3}\sqrt{2/p_1}.$$

Then, by integrating (4.13), substituting (4.12) and collecting the terms proportional to $\partial\Phi/\partial x$ and $\partial I/(3I\partial x)$, we find

$$U = U_\Phi \frac{\partial \Phi}{\partial x} + U_I \frac{1}{3I}\frac{\partial I}{\partial x} \quad \text{for } z - z_0 \gg 1, \tag{4.15}$$

with

$$U_\Phi = \int_0^\infty \int_\infty^z \left(\frac{g(s,z_0)}{g_1(0,z_0)} \left[\frac{2}{s+A} - G(s,z_0) \right] + \int_s^\infty \frac{g(p,z_0)}{g_1(0,z_0)}\,\mathrm{d}p \frac{\partial}{\partial s}\left[\frac{2}{s+A} - G(s,z_0) \right] \right) \mathrm{d}s\mathrm{d}z, \tag{4.16}$$

$$U_I = \int_0^\infty \int_\infty^z \left(\left[G - \frac{2}{s+A} \right]^2 - \frac{\partial}{\partial s}\left[G - \frac{2}{s+A} \right] + \frac{2A}{s+A}\left[\frac{\partial G}{\partial s} - \frac{1}{s+A} \right] \right) \mathrm{d}s\mathrm{d}z + U_\Phi. \tag{4.17}$$

Here,

$$g(z,z_0) \stackrel{\text{def}}{=} \frac{\partial G}{\partial z_0} \quad g_1(z,z_0) \stackrel{\text{def}}{=} \int_z^\infty g(z,z_0)\,\mathrm{d}z. \tag{4.18a,b}$$

Let us note that in (4.17) there is one term quadratic in G, whereas all other terms in (4.16), (4.17) are linear in G.

In order to simplify (4.16), (4.17), we refer to the smallness of parameter $A = O(\varepsilon^{1/3}) \ll 1$ which yields, taking into account (3.52*a*, *b*),

$$U_\Phi = \int_0^\infty \int_\infty^z \left[\frac{g}{g_1(0,z_0)} \left(\frac{2}{s} - G \right) + \frac{\partial G}{\partial s} g_1 + \frac{2}{(s+A)^2} \left(\frac{1}{s+1} - \frac{g_1}{g_1(0,z_0)} \right) \right] \mathrm{d}s\mathrm{d}z - 2(1 + \ln A), \tag{4.19}$$

$$U_I = \int_0^\infty \int_\infty^z \left(G^2 - \frac{4G}{z} - 2\frac{\partial G}{\partial s} - \frac{g[G - 2/s]}{g_1(0,z_0)} + \left[1 - \frac{g_1}{g_1(0,z_0)} \right] \frac{\partial}{\partial s}\left[G - \frac{2}{s} \right] \right) \mathrm{d}s\mathrm{d}z. \tag{4.20}$$

Let us examine (4.15)–(4.17) for $z_0 \ll -1$. For this purpose, let us keep the leading-order terms in the expansion of the respective integrands. Then, using thick QE–EDL solution (3.45*a*), we obtain that from (3.50), (4.18*a*) for $z_0 \ll -1$

$$G(z,z_0) = \frac{2}{z} - 4\sqrt{-z_0}\,\frac{\exp(-\sqrt{-z_0}z)}{1 - \exp(-2\sqrt{-z_0}z)} - \frac{1}{z - z_0}, \tag{4.21}$$

and,

$$g(z,z_0) = \frac{2\exp(-\sqrt{-z_0}z)}{1 - \exp(-2\sqrt{-z_0}z)} \left(\frac{1}{\sqrt{-z_0}} - z\frac{1 + \exp(-2\sqrt{-z_0}z)}{1 - \exp(-2\sqrt{-z_0}z)} \right) - \frac{1}{(z - z_0)^2}. \tag{4.22}$$

Integration of (4.22) yields

$$g_1(0,z_0) = \frac{2}{z_0}, \qquad g_1(z,z_0) = -\frac{1}{z - z_0} - \frac{2}{\sqrt{-z_0}}\,\frac{z\exp(-\sqrt{-z_0}z)}{1 - \exp(-2\sqrt{-z_0}z)}. \tag{4.23a,b}$$

By substituting (4.21)–(4.23*a*, *b*) into (4.16), (4.17), keeping the leading-order terms in the results of the integration and using (3.45*b*), we find:

$$U_\Phi = -2\ln 2 - \zeta_q, \quad U_I = 6\ln 2, \tag{4.24a,b}$$

and, thus, from (4.15)

$$U = 2\ln 2\left(\frac{\partial \ln I}{\partial x} - \frac{\partial \Phi}{\partial x}\right) - \zeta_q \frac{\partial \Phi}{\partial x} \text{ in Q1DL} \cap \text{QEB}. \tag{4.25}$$

Taking into account (3.8), (3.11) and the negativity of z_0, (4.25) yields the limiting Dukhin's type quasi-equilibrium slip (see Dukhin & Derjaguin 1976; Zholkovskij *et al.* 1996)

$$U = 2\ln 2 \frac{\partial}{\partial x}(\ln c - \varphi) - \zeta_q \frac{\partial \Phi}{\partial x} \text{ in Q1DL} \cap \text{QEB}. \tag{4.26}$$

By matching the slip formula (4.15) with the following quasi-equilibrium one, valid for $|\zeta| = O(1)$ ($-y_0 = O(1)$, compare with (2.38))

$$U = -2\ln \frac{1+\exp(\zeta_q)}{2} \frac{\partial}{\partial x}(\ln c - \varphi) - \zeta_q \frac{\partial \Phi}{\partial x},$$

we obtain, using (3.42), the following composite expression for the reduced slip velocity valid for any ζ in Q1DL $\cap$ QEB

$$U = U_\Phi \frac{\partial \Phi}{\partial x} + U_I \frac{1}{3}\frac{\partial \ln I}{\partial x} - 2\ln\left(1+\exp\left[\left(\zeta - \ln\frac{2p_1}{I}\right)/2\right]\right)\frac{\partial}{\partial x}(\ln I - \Phi). \tag{4.27}$$

Let us analyse in more detail this formula for the developed microscopic non-equilibrium space charge regime (3.56)–(3.60) ($1 < O(z_0) < \varepsilon^{-2/3}$, $4/3|\ln\varepsilon| < O(|\zeta|) < 1/\varepsilon$). According to (3.21*a*), for $1 < O(z) < z_0$, the leading-order term in the expansion of function G is

$$G = -\sqrt{2(z_0 - z)}, \tag{4.28}$$

and, thus,

$$g = -\frac{1}{\sqrt{2(z_0 - z)}}. \tag{4.29}$$

Integrating (4.22) and keeping the leading-order terms, we find

$$g_0 = -\sqrt{2z_0}, \quad g_1 = -\sqrt{\frac{1}{2(z_0 - z)}} \quad (1 < O(z) < z_0). \tag{4.30a,b}$$

Then, by substituting (4.28)–(4.30*a*, *b*) into (4.5), (4.15), (4.19), (4.20) and keeping the leading-order terms, we finally recover the extreme non-equilibrium electro-osmotic slip formula, for $4/3|\ln\varepsilon| < O(|\zeta|) < 1/\varepsilon$

$$u = \left(\zeta - \tfrac{4}{3}\ln\varepsilon\right)\frac{\partial \Phi}{\partial x} - \frac{\left(\zeta - \frac{4}{3}\ln\varepsilon\right)^2}{8}\frac{\partial \ln I}{\partial x} \quad \text{in Q1DL} \cap \text{QEB}, \tag{4.31}$$

in accord with Rubinstein *et al.* (2005).

Finally, in figure 13 we depict the dependence of the electro-osmotic factors U_Φ, U_I on ζ. We note the change of sign of U_I upon the decrease of ζ and transition from the quasi-equilibrium to the non-equilibrium EDL.

4.3. *Two-dimensional limiting electroconvection problem*

We turn now to formulation of the QEB flow problem to be solved in the domain $\{-\infty < x < \infty,\ 0 < y < 1,\ t > 0\}$. In order to return from the reduced slip velocity (4.2) to the total one we have to specify the outer edge y_1 of the EDL in (4.5) for non-equilibrium regimes (the term yU' in (4.5) is negligibly small for quasi-equilibrium regimes, $z_0 \ll -O(1)$). Based on (3.70), we identify y_1 with $\max(0, y_0)$.

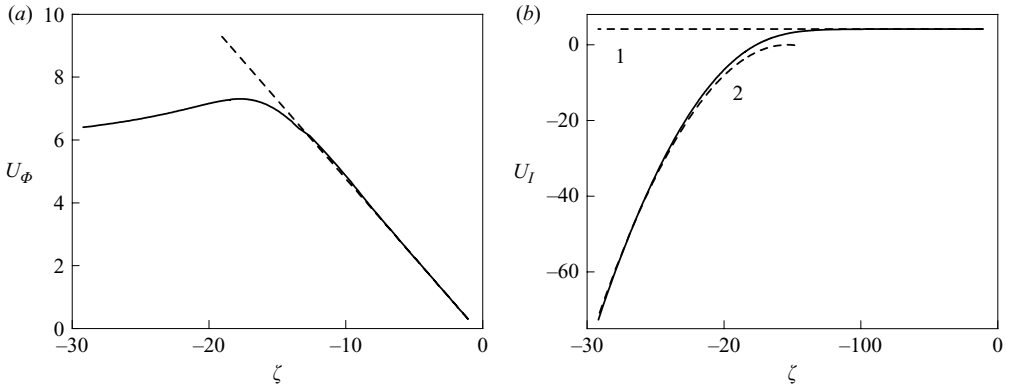

FIGURE 13. Dependence of electro-osmotic factors U_Φ, U_I on ζ. (a) —, U_Φ versus ζ; - - -, quasi-equilibrium asymptotics (4.24a); (b); — U_I versus ζ; - - - 1, quasi-equilibrium asymptotics (4.24b); - - - 2, non-equilibrium asymptotics (4.31).

This identification is, thus, an interpolation of the rigorous estimates of y_1 valid for developed non-equilibrium ($z_0 \gg 1$, $O(\zeta) < (4/3)\ln|\varepsilon|$) and quasi-equilibrium regimes ($z_0 \ll -1$, $O(\zeta) > (4/3)\ln|\varepsilon|$)) onto intermediate ones. Setting $y = \max(0, y_0)$ in (4.5) and using (4.27) we find

$$\begin{aligned}\overline{u}(x,0,t) - \varepsilon^{2/3} I^{-1/3}\max(0,z_0)\left[\frac{\partial \overline{u}}{\partial y}(x,0,t) + \frac{\partial \overline{\varphi}}{\partial y}(x,0,t)\frac{\partial \Phi}{\partial x}(x,t)\right]\\ = (U_\Phi + [-V - \varphi(x,0,t)])\frac{\partial \Phi}{\partial x}(x,t) + \frac{U_I}{3}\frac{\partial \ln I}{\partial x}(x,t)\\ - 2\ln\left(1 + \exp\left[\left(-V - \Phi(x,t) - \ln\frac{2p_1}{I}\right)\Big/ 2\right]\right)\frac{\partial}{\partial x}(\ln I - \Phi(x,t)).\end{aligned} \tag{4.32}$$

The rest of the universal limiting electroconvection formulation reads

$$\frac{\partial \overline{c}}{\partial t} + Pe(\overline{\boldsymbol{v}}\cdot\nabla)\overline{c} = \Delta\overline{c}, \tag{4.33}$$

$$\frac{D-1}{D+1}\Delta\overline{c} + \nabla\cdot(\overline{c}\nabla\overline{\varphi}) = 0, \tag{4.34}$$

$$\frac{1}{Sc}\frac{\partial \overline{\boldsymbol{v}}}{\partial t} = -\nabla p + \nabla\overline{\varphi}\Delta\overline{\varphi} + \Delta\overline{\boldsymbol{v}}, \tag{4.35}$$

$$\nabla\cdot\overline{\boldsymbol{v}} = 0, \qquad \overline{\boldsymbol{v}} = \overline{u}\widehat{\boldsymbol{i}} + \overline{w}\widehat{\boldsymbol{j}}; \tag{4.36}$$

$$\ln\overline{c}(x,0,t) + \overline{\varphi}(x,0,t) = \ln p_1 - V - \frac{(2\max(z_0,0))^{3/2} I^{1/2}}{3}, \tag{4.37}$$

$$\ln\overline{c}(x,1,t) + \overline{\varphi}(x,1,t) = \ln p_1, \qquad \frac{\partial \overline{c}}{\partial y} - \overline{c}\frac{\partial \overline{\varphi}}{\partial y}\bigg|_{y=0,1} = 0, \tag{4.38a, b}$$

$$\overline{u}(x,1,t) = 4\ln\frac{1+\exp(-\overline{\varphi}(x,1,t))}{2}\frac{\partial \overline{\varphi}}{\partial x}(x,1,t), \quad \overline{w}|_{y=0,1} = 0. \tag{4.39a, b}$$

Once more, the current density $I(x,t)$, the regular potential $\Phi(x,t)$ and the electro-osmotic factors U_Φ and U_I are given by, respectively, (3.79), (3.80) and (4.19), (4.20), whereas the control parameter z_0 is a solution of (3.54).

5. Linear stability of quiescent concentration polarization in the universal electro-osmotic formulation

It was shown in Rubinstein & Zaltzman (2000, 2001) that the non-equilibrium electro-osmosis, induced by the extended space charge of a strongly non-equilibrium EDL, renders the quiescent conduction unstable. Below, we employ the universal electro-osmotic slip theory of the previous section to explore this instability, in particular, to determine the precise critical parameter values for its onset. It is shown that the limiting formulation analysed is free of short-wave singularity which paves the way for the numerical study of the full nonlinear electro-osmotically driven electroconvection problem, which is difficult for a direct numerical solution in a realistic parameter range. Such a numerical study, including the exploration of the overlimiting conductance phenomenon, will be the subject of our forthcoming paper.

Let us analyse the linear stability of the following quiescent concentration polarization solution

$$c_0(y) = \frac{I_0}{2}\left(y - \tfrac{1}{2}\right) + 1, \quad \varphi_0(y) = \ln \frac{p_1\,[I_0/2\,(y-1/2)+1]}{(1+I_0/4)^2}, \tag{5.1a,b}$$

$$\boldsymbol{v}_0 = u_0\widehat{\boldsymbol{i}} + w_0\widehat{\boldsymbol{j}} = 0, \quad \Phi_0 = \ln \frac{I_0 p_1}{2\,(1+I_0/4)^2} \quad (0 < y < 1), \tag{5.2a,b}$$

to the regular limiting electroconvection problem (4.32)–(4.39a,b). Here, for $z_0 < 0$, the current density $I_0 = I_0(V)$ is given by

$$I_0 = 4\frac{1-\mathrm{e}^{-V/2}}{1+\mathrm{e}^{-V/2}}, \tag{5.3}$$

whereas for $z_0 > 0$ it is found through the solution of the equations

$$2\ln\frac{1-I_0/4}{1+I_0/4} = -V - \frac{(2\max(z_0,0))^{3/2} I_0^{1/2}}{3}, \tag{5.4}$$

$$P(z_0) + \tfrac{4}{3}\ln\varepsilon = -V - \ln\frac{I_0^{4/3}}{(1+I_0/4)^2}, \tag{5.5}$$

with $P(z_0)$ given by (3.55). The linearized problem for the perturbations c_1, φ_1 and $\boldsymbol{v}_1 = u_1\widehat{\boldsymbol{i}} + w_1\widehat{\boldsymbol{j}}$ of the solution (5.1a,b)–(5.5)

$$\frac{\partial c_1}{\partial t} + Pe\frac{I_0}{2}w_1 = \Delta c_1 \quad (t > 0,\ |x| < 0 < y < 1), \tag{5.6}$$

$$\frac{D-1}{D+1}\Delta c_1 + \nabla\cdot(c_0\nabla\varphi_1) + \frac{\partial}{\partial y}\left(c_1\frac{\mathrm{d}\varphi_0}{\mathrm{d}y}\right) = 0, \tag{5.7}$$

$$\frac{1}{Sc}\frac{\partial}{\partial t}\Delta w_1 = \Delta^2 w_1 + \frac{\partial^2\Delta\varphi_1}{\partial x^2}\frac{\mathrm{d}\varphi_0}{\mathrm{d}y} - \frac{\mathrm{d}^3\varphi_0}{\mathrm{d}y^3}\frac{\partial^2\varphi_1}{\partial x^2}; \tag{5.8}$$

$$\frac{\partial c_1}{\partial y}(x,0,t) - c_0(0)\frac{\partial\varphi_1}{\partial y}(x,0,t) - c_1(x,0,t)\frac{\mathrm{d}\varphi_0}{\mathrm{d}y}(0) = 0, \tag{5.9}$$

$$\begin{aligned}\frac{c_1(x,0,t)}{c_0(0)} + \varphi_1(x,0,t) = {} & -\frac{(2\max(z_0,0))^{3/2}}{3I_0^{1/2}}\frac{\partial c_1}{\partial y}(x,0,t) \\ & - \frac{(2\max(z_0,0))^{1/2} I_0^{1/2}}{P'(z_0)}\left(\frac{c_1(x,0,t)}{c_0(0)} - \frac{8}{3I_0}\frac{\partial c_1}{\partial y}(x,0,t) - \varphi_1(x,0,t)\right),\end{aligned} \tag{5.10}$$

$$\left(\frac{\partial^2 w_1}{\partial y^2}(x,0,t)-\frac{\mathrm{d}\varphi_0}{\mathrm{d}y}(0)\left[\frac{\partial^2\varphi_1}{\partial x^2}(x,0,t)-\frac{1}{c_0(0)}\frac{\partial^2 c_1}{\partial x^2}(x,0,t)+\frac{2}{I_0}\frac{\partial^3 c_1}{\partial x^2\partial y}(x,0,t)\right]\right)$$
$$\times\frac{\varepsilon^{2/3}\max(z_0,0)}{I_0^{1/3}}-\frac{\partial w_1}{\partial y}(x,0,t)=[U_\Phi(z_0)-V-\varphi_0(0)]$$
$$\times\left[\frac{\partial^2\varphi_1}{\partial x^2}(x,0,t)-\frac{1}{c_0(0)}\frac{\partial^2 c_1}{\partial x^2}(x,0,t)+\frac{2}{I_0}\frac{\partial^3 c_1}{\partial x^2\partial y}(x,0,t)\right]+U_I(z_0)$$
$$+\frac{2}{3I_0}\frac{\partial^3 c_1}{\partial x^2\partial y}(x,0,t)-2\ln\left(1+\frac{1+I_0/4}{p_1}e^{-\frac{V}{2}}\right)\frac{\partial^2}{\partial x^2}\left(\frac{c_1(x,0,t)}{c_0(0)}-\varphi_1(x,0,t)\right), \tag{5.11}$$

$$\frac{c_1(x,1,t)}{c_0(1)}+\varphi_1(x,1,t)=0, \tag{5.12}$$

$$\frac{\partial c_1}{\partial y}(x,1,t)-c_0(1)\frac{\partial\varphi_1}{\partial y}(x,1,t)-c_1(x,1,t)\frac{\mathrm{d}\varphi_0}{\mathrm{d}y}(1)=0, \tag{5.13}$$

$$w_1(x,0,t)=0,\quad w_1(x,1,t)=0, \tag{5.14a,b}$$

$$\frac{\partial w_1}{\partial y}(x,1,t)=-4\ln\frac{p_1+I_0/4+1}{2p_1}\frac{\partial^2\varphi_1}{\partial x^2}(x,1,t). \tag{5.15}$$

Equations (5.6)–(5.15) yield the spectral problem of the form

$$\lambda\xi+Pe\frac{I_0}{2}\omega=\frac{\mathrm{d}^2\xi}{\mathrm{d}y^2}-k^2\xi\qquad(0<y<1), \tag{5.16}$$

$$\frac{D-1}{D+1}\left(\frac{\mathrm{d}^2\xi}{\mathrm{d}y^2}-k^2\xi\right)+c_0\left(\frac{\mathrm{d}^2\psi}{\mathrm{d}y^2}-k^2\psi\right)+\frac{I_0}{2}\frac{\mathrm{d}\psi}{\mathrm{d}y}+\frac{\mathrm{d}}{\mathrm{d}y}\left(\frac{\mathrm{d}\varphi_0}{\mathrm{d}y}\xi\right)=0, \tag{5.17}$$

$$\frac{\mathrm{d}^4\omega}{\mathrm{d}y^4}-\left(2k^2+\frac{\lambda}{Sc}\right)\frac{\mathrm{d}^2\omega}{\mathrm{d}y^2}+\left(k^4+\frac{\lambda k^2}{Sc}\right)\omega=k^2\left[\left(\frac{\mathrm{d}^2\psi}{\mathrm{d}y^2}-k^2\psi\right)\frac{\mathrm{d}\varphi_0}{\mathrm{d}y}-\frac{\mathrm{d}^3\varphi_0}{\mathrm{d}y^3}\psi\right], \tag{5.18}$$

$$\frac{\xi(0)}{c_0(0)}+\psi(0)=-\frac{(2\max(z_0,0))^{3/2}}{3I_0^{1/2}}\frac{\mathrm{d}\xi}{\mathrm{d}y}(0)$$
$$-\frac{\sqrt{2\max(z_0,0)}I_0^{1/2}}{P'(z_0)}\left(\frac{\xi(0)}{c_0(0)}-\frac{8}{3I_0}\frac{\mathrm{d}\xi}{\mathrm{d}y}(0)-\psi(0)\right), \tag{5.19}$$

$$\frac{\mathrm{d}\xi}{\mathrm{d}y}(0)-c_0(0)\frac{\mathrm{d}\psi}{\mathrm{d}y}(0)-\xi(0)\frac{\mathrm{d}\varphi_0}{\mathrm{d}y}(0)=0, \tag{5.20}$$

$$\frac{\varepsilon^{2/3}\max(z_0,0)}{I_0^{1/3}}\left(\frac{\mathrm{d}^2\omega}{\mathrm{d}y^2}(x,0,t)+k^2\frac{\mathrm{d}\varphi_0}{\mathrm{d}y}(0)\left[\psi(0)-\frac{\xi(0)}{c_0(0)}+\frac{2}{I_0}\frac{\mathrm{d}\xi}{\mathrm{d}y}(0)\right]\right)$$
$$-\frac{\mathrm{d}\omega}{\mathrm{d}y}(x,0,t)=-k^2[U_\Phi(z_0)-V-\varphi_0(0)]\left[\psi(0)-\frac{\xi(0)}{c_0(0)}+\frac{2}{I_0}\frac{\mathrm{d}\xi}{\mathrm{d}y}(0)\right]$$
$$-U_I(z_0)\frac{2k^2}{3I_0}\frac{\mathrm{d}\xi}{\mathrm{d}y}(0)+2k^2\left(\frac{\xi(0)}{c_0(0)}-\psi(0)\right)\ln\left(1+\frac{1+I_0/4}{p_1}\exp(-V/2)\right), \tag{5.21}$$

$$\frac{\xi(1)}{c_0(1)}+\psi(1)=0, \tag{5.22}$$

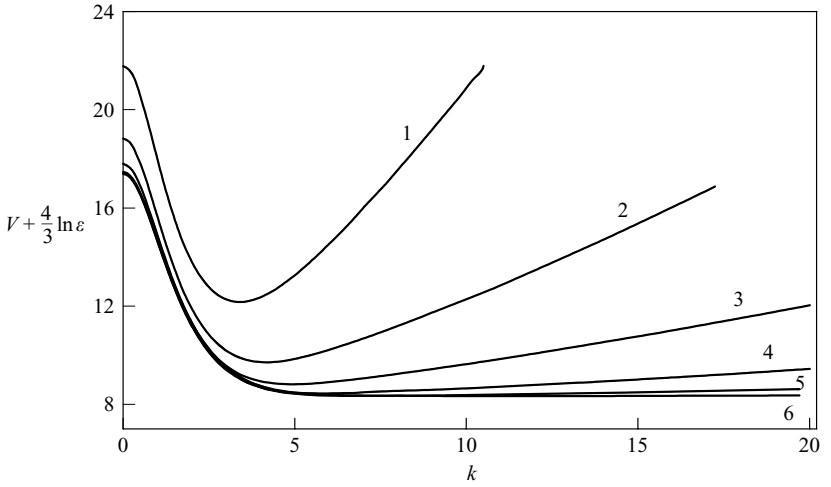

FIGURE 14. Marginal stability curves (voltage V versus wavenumber k) for universal electro-osmotic formulation for $Pe=0.5$, $D=1$, $p_1=4$ and six values of ε: 1, -10^{-2}; 2, -3×10^{-3}; 3, -10^{-3}; 4, -3×10^{-4}; 5, -10^{-4}; 6, -3×10^{-6}.

$$\frac{\mathrm{d}\xi}{\mathrm{d}y}(1)-c_0(1)\frac{\mathrm{d}\psi}{\mathrm{d}y}(1)-\xi(1)\frac{\mathrm{d}\varphi_0}{\mathrm{d}y}(1)=0, \tag{5.23}$$

$$\omega(0)=0, \quad \omega(1)=0, \tag{5.24a,b}$$

$$\frac{d\omega}{\mathrm{d}y}(1)=4k^2\ln\frac{p_1+1+I_0/4}{2p_1}\psi(1). \tag{5.25}$$

Here ξ, ψ and ω are the Fourier transforms

$$\xi(y)=\int_{-\infty}^{\infty}\mathrm{e}^{\mathrm{i}kx}\overline{c}_1(x,y)\,\mathrm{d}x, \tag{5.26}$$

$$\psi(y)=\int_{-\infty}^{\infty}\mathrm{e}^{\mathrm{i}kx}\overline{\varphi}_1(x,y)\,\mathrm{d}x, \tag{5.27}$$

$$\omega(y)=\int_{-\infty}^{\infty}\mathrm{e}^{\mathrm{i}kx}\overline{w}_1(x,y)\,\mathrm{d}x, \tag{5.28}$$

of the spatial factors $\overline{c}_1$, $\overline{\varphi}_1$, $\overline{w}_1$ in the representation

$$c_1(x,y,t)=\overline{c}_1(x,y)\,\mathrm{e}^{\lambda t}, \tag{5.29}$$

$$\varphi_1(x,y,t)=\overline{\varphi}_1(x,y)\,\mathrm{e}^{\lambda t} \tag{5.30}$$

$$w_1(x,y,t)=\overline{w}_1(x,y)\,\mathrm{e}^{\lambda t}. \tag{5.31}$$

where k is the wavenumber and λ is the spectral parameter – linear growth rate ($\mathrm{Re}\lambda>0$ implies instability of solution (5.6)–(5.15)).

Below are the results of a numerical solution of the spectral problem (5.16)–(5.25). Thus, in figure 14 we present the marginal stability curves in the V/k plane for $Pe=0.5$, $D=1$, $p_1=4$ and six values of $\varepsilon=10^{-2}$, 3×10^{-3}, 10^{-3}, 3×10^{-4}, 10^{-4}, 3×10^{-5}. It can be seen that the minimum in the V_{cr} versus k curve is more pronounced the larger ε is. In figure 15, we present the ε-dependence of the threshold V_{cr} for $Pe=0.5$, $D=1$, $p_1=4$ in the limiting electroconvective formulation

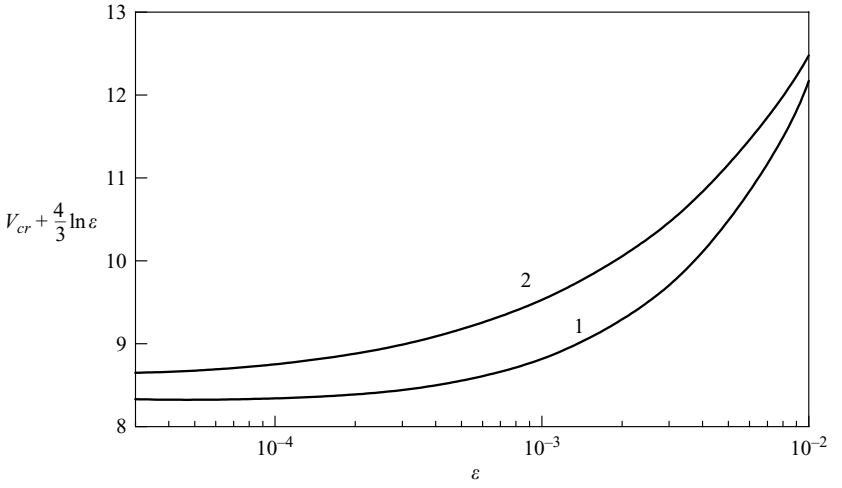

FIGURE 15. The ε-dependence of the voltage threshold V_{cr} for $Pe=0.5$, $D=1$, $p_1=4$ in: 1, – universal electro-osmotic formulation, and 2, full electroconvective formulation.

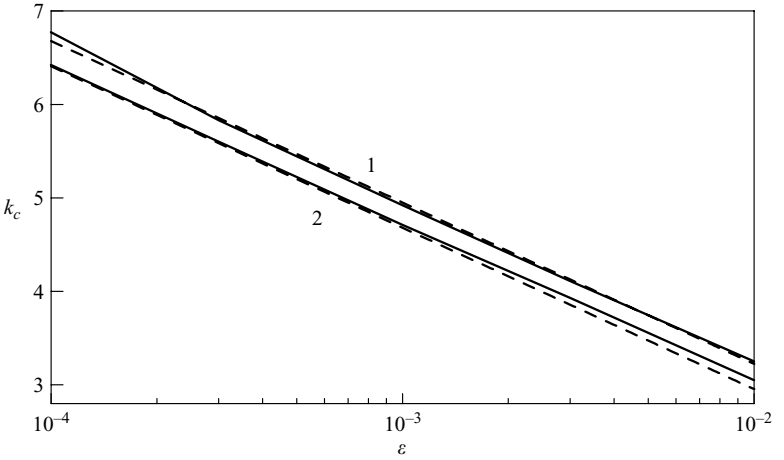

FIGURE 16. The ε-dependence of the critical wavenumber k_{cr} for $Pe=0.5$, $D=1$, $p_1=4$ in: 1, — universal electroosmotic formulation; - - -, empirical formula (5.32), and 2, — full electroconvective formulation; - - -, empirical formula (6.18).

(4.32)–(4.39a,b). In figure 16, we present the corresponding ε-dependence of the critical wavenumber k_c for this formulation with the same parameter values as in previous figure, (continuous line 1), whereas dashed line 1 stands for the analytical approximation of this dependence by the empirical formula

$$k_{cr} \simeq -0.25 - \tfrac{3}{4}\ln\varepsilon. \tag{5.32}$$

Finally, in figure 17, we present the dependence of the threshold V_{cr} on the relative diffusivity D for $\varepsilon=3\times10^{-5}$.

We conclude this section by noting that for very large wavenumbers $k\gg1/\varepsilon$ the quiescent concentration polarization solution is stable, with perturbations decaying

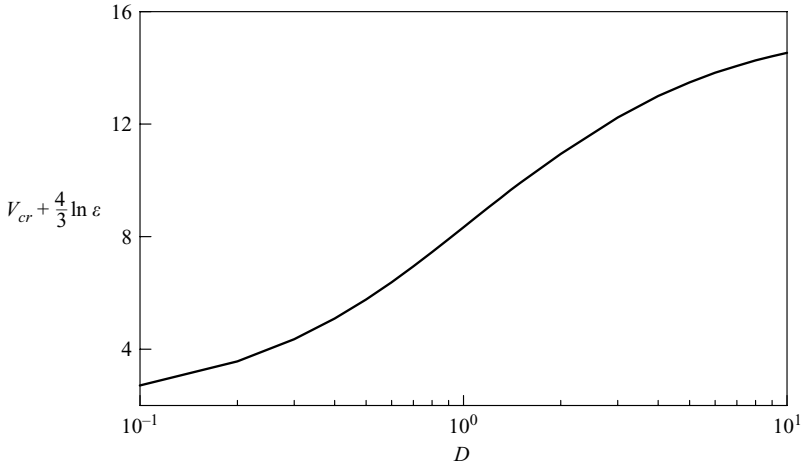

FIGURE 17. The voltage threshold V_{cr} dependence on the relative diffusivity D in the universal electro-osmotic formulation for $Pe=0.5$, $p_1=4$, $\varepsilon=3\times10^{-5}$.

as

$$\lambda \simeq -k^2, \tag{5.33}$$

that is in a fashion typical of diffusion. This is the ultimate expression of the absence of the short-wave singularity from the electro-osmotic formulation (4.32)–(4.39a,b). Estimate (5.33) follows from the short-wave ($k \gg 1/\varepsilon$) asymptotic analysis of problem (5.16)–(5.25) based upon defining a small parameter $\omega = k^{-1}$ and observing that for $\omega \ll 1$, (5.16)–(5.25) are singularly perturbed with two boundary layers at $y=0$, 1. Straightforward asymptotic boundary-layer analysis of this problem yields for $k \gg 1$ the leading-order solution of the form:

$$\xi = 1 - y + O\left(\frac{1}{k^2}\right), \quad \psi = \frac{1-D}{(1+D)\,\bar{c}_0(y)}(1-y) + O\left(\frac{1}{k^2}\right),$$

$$\omega = O(1)\,\mathrm{e}^{-y/k}, \quad \lambda \simeq -k^2 + O\left(\frac{1}{k^2}\right) \quad (0 < y < 1).$$

6. Linear stability of quiescent concentration polarization in the full electroconvective formulation

In this section we deal with linear stability analysis of the quiescent concentration polarization solution in the full electroconvective formulation (2.1)–(2.5), (2.8)–(2.13). In order to simplify the full formulation (2.1)–(2.5), (2.8)–(2.13) and to avoid the detailed study of the double electric layer at the 'enriched' anodic membrane's surface ($y=1$) we assume there local electroneutrality with local equilibrium and quasi-equilibrium electro-osmotic slip of the kind (4.1) which yields boundary conditions of the form:

$$\mu^+(x,1,t) = \ln p_1, \quad \mu_y^-(x,1,t) = 0, \quad \varphi(x,1,t) = \frac{\ln p_1 - \mu^-(x,1,t)}{2}, \tag{6.1a–c}$$

$$u(x,1,t) = -2\ln\frac{\sqrt{p_1} + e^{\mu^-(x,1,t)/2}}{2\sqrt{p_1}}\mu_x^-(x,1,t), \quad w(x,1,t) = 0. \tag{6.2a,b}$$

Here, μ^+ and μ^- are the cationic and anionic electrochemical potentials. Conditions (6.1*a*, *b*) imply local equilibrium for cations at the membrane–solution interface and impermeability of the latter for anions, whereas (6.1*c*) and (6.2*a*) imply, respectively, the local electroneutrality and the limiting quasi-equilibrium electroosmotic slip.

The quiescent steady-state concentration polarization solution $\mu_0^{\pm}$, φ_0, $\boldsymbol{v}_0$, p_0 whose stability we are about to study is found numerically from the following one-dimensional boundary-value problem:

$$\frac{\mathrm{d}}{\mathrm{d}y}\left(\exp(\mu_0^+ - \varphi_0)\frac{\mathrm{d}\mu_0^+}{\mathrm{d}y}\right) = 0, \quad \varepsilon^2\frac{\mathrm{d}^2\varphi_0}{\mathrm{d}y^2} = \exp(\mu_0^- + \varphi_0) - \exp(\mu_0^+ - \varphi_0) \quad (0 < y < 1),$$

$$\mu_0^+(0) = \ln p_1 - V, \quad \varphi_0(0) = -V,$$

$$\mu_0^+(1) = \ln p_1, \quad \varphi_0(1) = \tfrac{1}{2}\ln\left(p_1\int_0^1 \exp(\varphi_0)\,\mathrm{d}y\right),$$

$$\mu_0^-(y) = \mu_0^+(1) - 2\varphi_0(1), \quad \boldsymbol{v}_0(y) = 0, \quad p_0(y) = \frac{1}{2}\left(\frac{\mathrm{d}\varphi_0}{\mathrm{d}y}\right)^2 + \text{const}.$$

The linearized problem for perturbations $\mu_1^{\pm}$, φ_1, $\boldsymbol{v}_1 = u_1\widehat{\boldsymbol{i}} + w_1\widehat{\boldsymbol{j}}$ is

$$\frac{\partial}{\partial t}(\mu_1^+ - \varphi_1) + Pew_1\frac{\mathrm{d}}{\mathrm{d}y}(\mu_0^+ - \varphi_0) = \frac{D+1}{2}\left[\Delta\mu_1^+ + (\mu_1^+ - \varphi_1)\frac{\mathrm{d}^2\mu_0^+}{\mathrm{d}y^2}\right.$$
$$\left. + \left(\frac{\partial}{\partial y}(\mu_1^+ - \varphi_1) + (\mu_1^+ - \varphi_1)\frac{\mathrm{d}}{\mathrm{d}y}(\mu_0^+ - \varphi_0)\right)\frac{\mathrm{d}\mu_0^+}{\mathrm{d}y} + \frac{\partial\mu_1^+}{\partial y}\frac{\mathrm{d}}{\mathrm{d}y}(\mu_0^+ - \varphi_0)\right], \tag{6.3}$$

$$\frac{\partial}{\partial t}(\mu_1^- + \varphi_1) + Pew_1\frac{\mathrm{d}\varphi_0}{\mathrm{d}y} = \frac{D+1}{2D}\left[\Delta\mu_1^- + \frac{\mathrm{d}\varphi_0}{\mathrm{d}y}\frac{\partial\mu_1^-}{\partial y}\right], \tag{6.4}$$

$$\varepsilon^2\Delta\varphi_1 = \exp(\mu_0^- + \varphi_0)(\mu_1^- + \varphi_1) - \exp(\mu_0^+ - \varphi_0)(\mu_1^+ - \varphi_1), \tag{6.5}$$

$$\frac{1}{Sc}\frac{\partial\Delta w_1}{\partial t} = \Delta^2 w_1 + \frac{\partial^2\Delta\varphi_1}{\partial x^2}\frac{\mathrm{d}\varphi_0}{\mathrm{d}y} - \frac{\mathrm{d}^3\varphi_0}{\mathrm{d}y^3}\frac{\partial^2\varphi_1}{\partial x^2}, \tag{6.6}$$

$$\mu_1^+\big|_{y=0,1} = 0, \quad \left.\frac{\partial\mu_1^-}{\partial y}\right|_{y=0,1} = 0, \quad \varphi_1|_{y=0} = 0, \tag{6.7a–c}$$

$$(2\varphi_1 + \mu_1^-)|_{y=1} = 0, \quad w_1|_{y=0,1} = 0, \quad \left.\frac{\partial w_1}{\partial y}\right|_{y=0} = 0, \tag{6.8a–c}$$

$$\left.\frac{\partial w_1}{\partial y}\right|_{y=1} = 2\ln\frac{\sqrt{p_1} + \exp(-\mu_0^-(1)/2)}{2\sqrt{p_1}}\frac{\partial^2\mu_1^-}{\partial x^2}(x, 1, t). \tag{6.9}$$

Equations (6.3)–(6.9) yield a spectral problem in the form

$$\frac{2Pe}{D+1}W\frac{\mathrm{d}}{\mathrm{d}y}(\mu_0^+ - \varphi_0) = \frac{\mathrm{d}^2M^+}{\mathrm{d}y^2} - k^2M^+ + \frac{\mathrm{d}\mu_0^+}{\mathrm{d}y}\frac{\mathrm{d}}{\mathrm{d}y}(M^+ - \Psi) + \frac{\mathrm{d}}{\mathrm{d}y}(\mu_0^+ - \varphi_0)$$
$$\times\frac{\mathrm{d}M^+}{\mathrm{d}y} - \left(\lambda\frac{D+1}{2D} - \frac{\mathrm{d}\mu_0^+}{\mathrm{d}y}\frac{\mathrm{d}}{\mathrm{d}y}(\mu_0^+ - \varphi_0) - \frac{\mathrm{d}^2\mu_0^{+\prime\prime}}{\mathrm{d}y^2}\right)(M^+ - \Psi), \tag{6.10}$$

$$\frac{2D}{D+1}PeW\frac{\mathrm{d}\varphi_0}{\mathrm{d}y}=\frac{\mathrm{d}^2M^-}{\mathrm{d}y^2}-k^2M^-+\frac{\mathrm{d}\varphi_0}{\mathrm{d}y}\frac{\mathrm{d}M^-}{\mathrm{d}y}-\lambda(M^-+\Psi), \tag{6.11}$$

$$\varepsilon^2\left(\frac{\mathrm{d}^2\Psi}{\mathrm{d}y^2}-k^2\Psi\right)=\exp(\mu_0^-+\varphi_0)(M^-+\Psi)-\exp(\mu_0^+-\varphi_0)(M^+-\Psi), \tag{6.12}$$

$$\frac{1}{k^2}\frac{\mathrm{d}^4W}{\mathrm{d}y^4}-\left(2+\frac{\lambda}{Sck^2}\right)\frac{\mathrm{d}^2W}{\mathrm{d}y^2}+\left(k^2+\frac{\lambda}{Sc}\right)W=\left(\frac{\mathrm{d}^2\Psi}{\mathrm{d}y^2}-k^2\Psi\right)\frac{\mathrm{d}\varphi_0}{\mathrm{d}y}-\Psi\frac{\mathrm{d}^3\varphi_0}{\mathrm{d}y^3}, \tag{6.13}$$

$$M^+|_{y=0,1}=0,\quad \frac{\mathrm{d}}{\mathrm{d}y}M^-\bigg|_{y=0,1}=0,\quad \Psi|_{y=0}=0, \tag{6.14a–c}$$

$$2\Psi(1)+M^-(1)=0,\quad W|_{y=0,1}=0,\quad \frac{\mathrm{d}W}{\mathrm{d}y}(0)=0, \tag{6.15a, b}$$

$$\frac{\mathrm{d}W}{\mathrm{d}y}(1)+2\ln\frac{\sqrt{p_1}+\exp\left(-\mu_0^-(1)/2\right)}{2\sqrt{p_1}}k^2M^-(1)=0. \tag{6.16}$$

Here, $\Psi(y,k)$, $M^{\pm}(y,k)$ $W(y,k)$ are the Fourier transforms of the spacial factors of perturbations of the electric potential, ionic electrochemical potentials and normal velocity, with k and λ being the wavenumber and linear growth rate, respectively, equivalent to those in (5.26)–(5.31).

We start with the analysis of the short-wave asymptotic behaviour ($k\gg 1/\varepsilon$) of λ in the problem (6.10)–(6.16) by considering asymptotic expansions of the form:

$$M^{\pm}=M_0^{\pm}(y)+O\left(\frac{1}{k^2}\right),\quad \Psi=\Psi_0(y)+\frac{\Psi_1(y)}{k^2}+O\left(\frac{1}{k^4}\right),$$

$$W=W_0(y)+O\left(\frac{1}{k^2}\right),\quad \lambda=\lambda_0k^2+\lambda_1\frac{D+1}{2D}+O\left(\frac{1}{k^2}\right).$$

By substituting these expansions into the spectral problem (6.10)–(6.16), we find that a non-trivial solution to the leading-order problem exists only if

$$\lambda_0=-\frac{2}{D+1}. \tag{6.17}$$

The corresponding leading-order solution is

$$M_0^-(y)=0,\quad \Psi_0(y)=0,\quad W_0(y)=0,\quad \Psi_1(y)=-\frac{\exp(\mu_0^-+\varphi_0)}{\varepsilon^2}M_0^+,$$

whereas λ_1 and $M_0^+(y)$ are obtained from the solution of the following eigenvalue problem

$$\frac{\mathrm{d}^2M_0^+}{\mathrm{d}y^2}+\frac{\mathrm{d}M_0^+}{\mathrm{d}y}\frac{\mathrm{d}}{\mathrm{d}y}\left(2\mu_0^+-\varphi_0\right)+\left[\frac{\mathrm{d}\mu_0^+}{\mathrm{d}y}\frac{\mathrm{d}}{\mathrm{d}y}\left(\mu_0^+-\varphi_0\right)+\frac{\exp(\mu_0^-+\varphi_0)}{\varepsilon^2}-\lambda_1\right]M_0^+=0,$$

$$M_0^+|_{y=0,1}=0.$$

Equation (6.17) implies once more that for very large wavenumbers, $k\gg 1/\varepsilon$, the quiescent concentration polarization solution is stable with perturbations decaying at a rate proportional to k^2, typical of diffusion. Below we present the results of a numerical solution of the spectral problem (6.10)–(6.16). Thus, in figure 18 we present

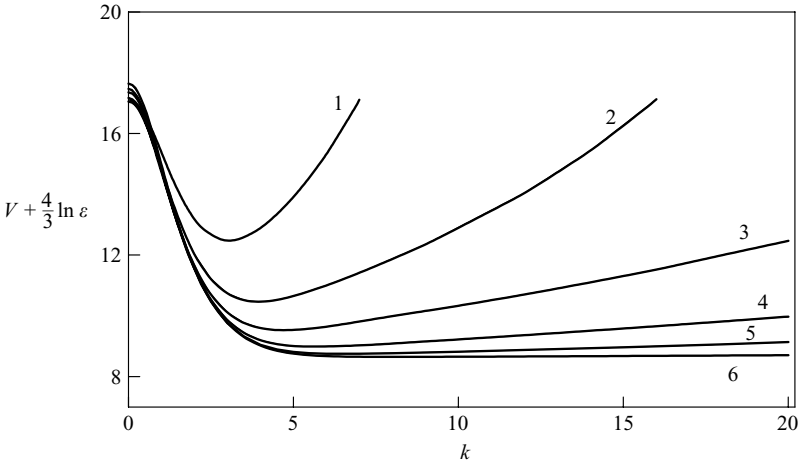

FIGURE 18. Marginal stability curves (voltage V versus wavenumber k) for the full electroconvective formulation for $Pe=0.5$, $D=1$, $p_1=4$ and six values of ε: 1, 10^{-2}; 2, 3×10^{-3}; 3, 10^{-3}; 4, 3×10^{-4}; 5, 10^{-4}; 6, 3×10^{-6}.

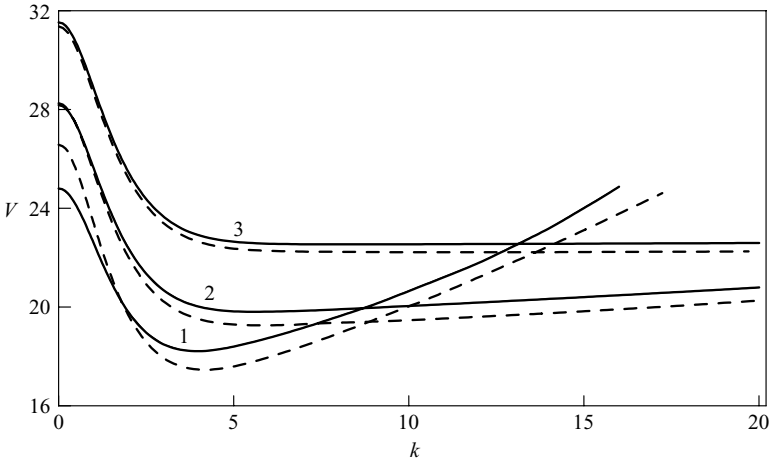

FIGURE 19. Comparison of marginal stability curves for the universal electroosmotic formulation (continuous lines) and the full electroconvective formulation (dashed lines) for $Pe=0.5$, $D=1$ and three values of ε: 1, 3×10^{-3}; 2, 3×10^{-4}; 3, 3×10^{-6}.

the marginal stability curves in the V/k plane for $Pe=0.5$, $D=1$, $p_1=4$ and six values of $\varepsilon=10^{-2}$, 3×10^{-3}, 10^{-3}, 3×10^{-4}, 10^{-4}, 3×10^{-5}. It can be seen that the minimum in the V_{cr} versus k curve is more pronounced the larger ε is. In figure 19, we compare the marginal V/k curve from figure 14 and 18 with $\varepsilon=3\times10^{-3}$, 3×10^{-4}, 3×10^{-5}. We note the close agreement between the marginal stability curve in the full formulation with $\varepsilon=3\times10^{-5}$ and that in the universal electro-osmotic formulation.

The ε-dependence of the threshold V_{cr} and the critical wavenumber k_c are presented in figures 15, 16 (lines 2), respectively, for $Pe=0.5$, $D=1$, $p_1=4$. Figure 16 shows the analytical fit of the critical wavenumber k_c by the expression (dashed line 2):

$$k_c=-\tfrac{3}{4}\ln\varepsilon-\tfrac{1}{2}. \tag{6.18}$$

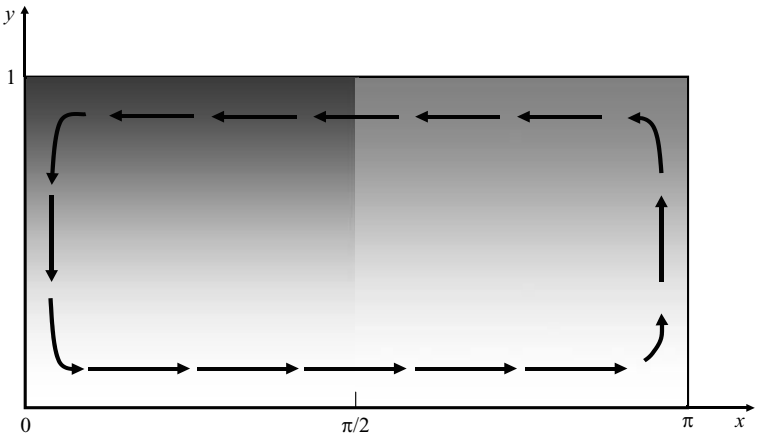

FIGURE 20. Sketch of a test vortex.

We note again that for small ε, the threshold values of the voltage V_{cr} and the critical wavenumber k_c closely agree in both formulations.

7. Instability mechanism

The essence of the described non-equilibrium electro-osmotic instability is rooted in the following peculiarity of the non-equilibrium space charge compared to that of the quasi-equilibrium EDL (see Appendix B). The total charge of the latter decreases upon the increase of the interface bulk concentration and so does its related space charge density (see (B 1), Appendix B). As opposed to this, the total charge of non-equilibrium EDL is essentially constant (see (B 2)). The extent of the non-equilibrium EDL is governed by the interface current density with interface concentration essentially zero, (3.81).

Given these basic features of the space charge, let us consider an accidental macroscopic 'test' vortex superimposed upon the basic quiescent concentration polarization steady state with electroneutral concentration decreasing towards the interface (see figure 20). The portion of this vortex descending towards the depleted wall brings the high bulk concentration to the interface, whereas the ascending part of the vortex does the opposite and brings the low interface concentration towards the bulk. For QE–EDL, this yields the decrease of the space charge density in the EDL at the 'descending' side of the flow and, correspondingly, decrease of the pressure. By the same mechanism, the pressure at the ascending side increases, thus, creating a lateral pressure drop which tends to decelerate the rotation. This is not so for non-equilibrium conditions. In this case, the increase of concentration in the descending part of the vortex, with the interface concentration remaining low, yields the increase of the interface current density. This, in turn, leads to compression of the extended space charge with its total value remaining unchanged. This results in the increase of the space charge density and the related increase of pressure (at the ascending side of the vortex, the opposite happens). The related lateral pressure drop, thus, tends to accelerate the rotation in the vortex which is the essence of the positive feedback in the described non-equilibrium electro-osmotic instability. This is shown in figure 21 in which we present the y- dependence of the lateral force terms in the perturbed Stokes equation (2.4) for the lateral velocity u_1, namely, the x-component of the negative

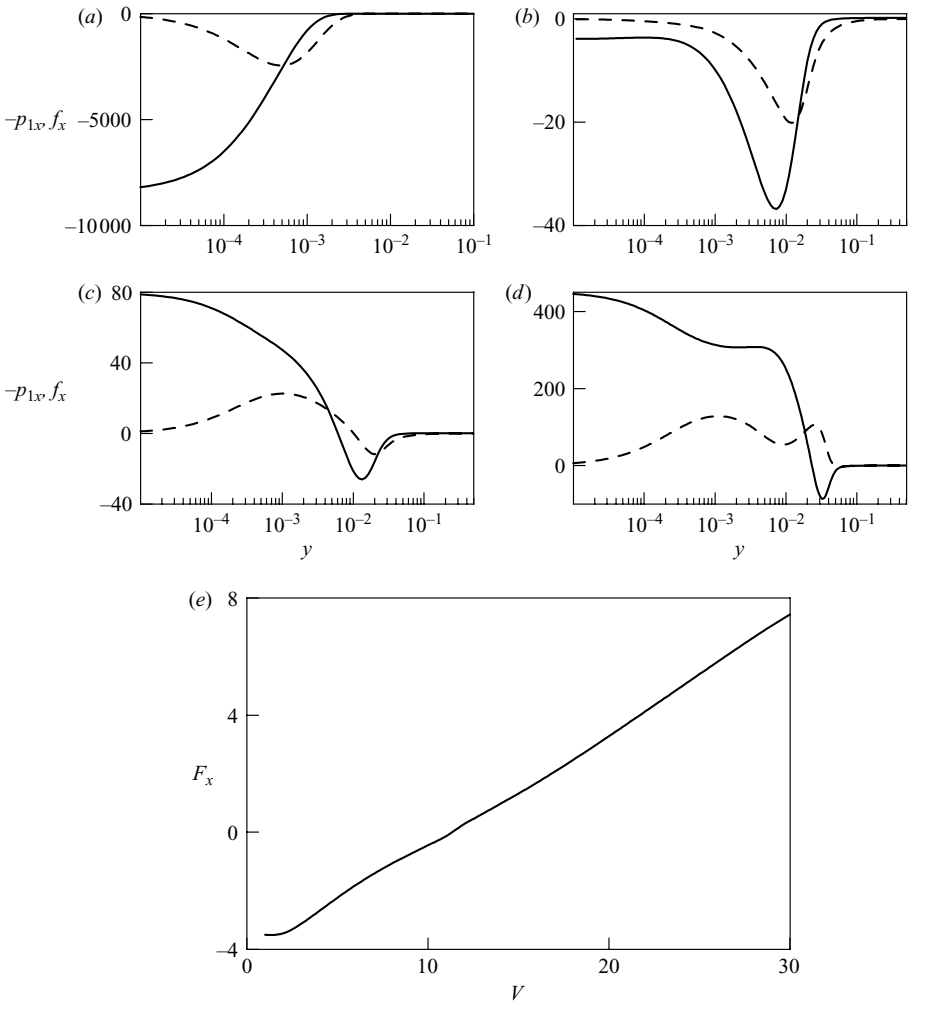

FIGURE 21. (*a*)–(*d*) The dependence of $-\partial p_1/\partial x$ (continuous lines) and f_x (dashed lines) on y for (*a*) $V=1$, (*b*) $V=10$, (*c*) $V=11$, (*d*) $V=20$, and $\varepsilon=10^{-3}$, $Pe=0.5$, $p_1=4$, $D=1$. (*e*) The dependence of the total lateral electric force F_x in the EDL on the voltage V for $\varepsilon=10^{-3}$, $Pe=0.5$, $p_1=4$, $D=1$.

pressure perturbation gradient

$$-\frac{\partial p_1}{\partial x}=-\frac{\partial^2\varphi_1}{\partial x\partial y}\frac{\mathrm{d}\varphi_0}{\mathrm{d}y}$$

and the x-component of the electric force perturbation

$$f_x \stackrel{\text{def}}{=} \frac{\partial\varphi_1}{\partial x}\frac{\mathrm{d}^2\varphi_0}{\mathrm{d}y^2},$$

as determined from the solution of the linearized problem (6.10)–(6.16):

$$-\frac{\partial p_1}{\partial x}=\mathrm{i}k\frac{\mathrm{d}\varphi_0}{\mathrm{d}y}\frac{\partial\Psi}{\partial y}\,\mathrm{e}^{-\mathrm{i}kx}\,\mathrm{e}^{\lambda t},\quad f_x=-\mathrm{i}k\frac{\mathrm{d}^2\varphi_0}{\mathrm{d}y^2}\Psi\,\mathrm{e}^{-\mathrm{i}kx}\,\mathrm{e}^{\lambda t}.$$

Thus, in figures 21(*a–d*) we present the dependence of $-\partial p_1/\partial x$ and f_x on y in the EDL calculated at the rotation axis $x=\pi/2$ of a counterclockwise rotating vortex for

$\varepsilon = 10^{-3}$, $k = 1$, $D = 1$, $Pe = 0.5$, $t = 0$ and a sequence of voltages $V = 1$, 10, 11, 20. In this example, the transition from stabilization to destabilization (figure 21*c,d*) by the local forces in the electric double layer occurs between $V = 10$ and $V = 11$. This is further illustrated in figure 21(*e*) in which we plot the overall lateral electric force F_x defined by (2.33) (equal, by (2.36), to minus the total lateral pressure gradient, $-P_x$) as a function of the applied voltage V. We note that this force indeed changes sign in the range $10 < V < 11$ upon the change of direction in which the local forces in the electric double layer are predominantly acting.

In kinematic terms, that is in terms of the electro-osmotic slip rather than force balance, the mechanism of the described instability is as follows. The increase of the interface concentration in the descending portion of the aforementioned seed vortex (amounting to increase of the local current density) results by the non-equilibrium slip condition (2.41) in a positive slip velocity, that is accelerated rotation. As opposed to this, owing to the opposite sign of the electro-osmotic factor in the quasi-equilibrium slip conditions (2.37)–(2.39), increase of the interface concentration results in a negative slip velocity that is a negative feedback and stability.

Appendix A. Calculation of parameter y_0 for $O(|\zeta|) < \frac{4}{3}|\ln\varepsilon|$

In the case of thin QE–EDL, the control parameter r_0 (or y_0) may be calculated by a straightforward integration of (3.23) over the interval $0 < r < \infty$ in the form:

$$\int_0^\infty \frac{2\mathrm{d}R}{\sqrt{R^2 - 4r_0}}\mathrm{d}r = -\int_0^\infty R\,\mathrm{d}r. \tag{A 1}$$

Equation (A 1) yields

$$2\ln(-R + \sqrt{R^2 + 4})\Big|_{r=0}^{r=\infty} = -\zeta_q(x),$$

and using (3.23) and boundary condition (3.24) we find that

$$2\ln 2 - 2\ln 2\sqrt{\frac{2p_1}{r_0}I^{-2/3}} = -\zeta_q(x),$$

where $\zeta_q(x)$ is the quasi-equilibrium ζ-potential defined by (3.39).

Using the same integration in the case of thick QE–EDL, we show that the contribution of the higher-order terms in the composite thick QE–EDL solution is negligible in the overall potential balance. Indeed, substituting the QE–EDL component of the composite solution (3.45*a*, *b*) into the overall potential drop across QE–EDL (3.39) yields

$$\int_0^\infty \left(\frac{Q(r/\sqrt{r_0})}{\sqrt{r_0}} + \frac{2}{r} + R(r)\right)\mathrm{d}r = \zeta_q(x).$$

Here $Q(q)$, given by (3.26), and $R(r)$, given by (3.30), are, respectively, the inner and outer components of the composite thick QE–EDL solution. Multiplication of (3.27) by $\mathrm{d}Q/\mathrm{d}q$ followed by integration over the interval (a, b) yields

$$\int_a^b \frac{Q(r/\sqrt{r_0})}{\sqrt{r_0}}\,\mathrm{d}r = -2\ln(|Q(r/\sqrt{r_0})|)\Big|_a^b \text{ for any } 0 < a < b. \tag{A 2}$$

Similar integration of (3.23) yields

$$\int_a^b R\,\mathrm{d}r = -\,2\ln(|R| + \sqrt{R^2+4})\Big|_a^b. \tag{A 3}$$

Superposition of (A 2) and (A 3) yields

$$\int_a^b \left(\frac{Q(r/\sqrt{r_0})}{\sqrt{r_0}} + \frac{2}{r} + R(r)\right)\mathrm{d}r = -2\ln\left(|Q(r/\sqrt{r_0})|\, r\,[|R| + \sqrt{R^2+4}]\right)\Big|_a^b. \tag{A 4}$$

Substituting the limits $a=0$ and $b=\infty$ into (A 4) and using (3.26), (3.31) we obtain

$$\int_0^\infty \left(\frac{Q(r/\sqrt{r_0})}{\sqrt{r_0}} + \frac{2}{r} + R(r)\right)\mathrm{d}r = \ln\frac{r_0 I^{2/3}}{2p_1}. \tag{A 5}$$

Finally, equating the left-hand side of (A 5) to $-\zeta_q(x)$, we recover (3.46) for the control parameter y_0. Thus, in spite of the approximate formula (3.45*b*) failing to hold point-wise for $\zeta = -O(1)$, it still provides the exact expression for y_0 for all values of ζ-potential in the range $O(1) \leqslant |\zeta| < (4/3)|\ln\varepsilon|$.

Appendix B. Relation between space charge and parameter y_0 (z_0)

Let us define the overall charge in Q1DL as

$$\Sigma \overset{\text{def}}{=} \int_0^\infty (c^+ - c^-)\,\mathrm{d}z = -I^{1/3}\varepsilon^{4/3}F(0)$$

and analyse its relation to parameter y_0 (or z_0) for all regimes of EDL. Equations (3.38), (3.45*b*) yield

$$\Sigma = \frac{\varepsilon}{\sqrt{2p_1}}(y_0 I + 2p_1) = \varepsilon\sqrt{\frac{2}{p_1}}\,(p_1 - \bar{c}(x,0,t)) \quad \text{for } O(|\zeta|) < \tfrac{4}{3}|\ln\varepsilon|. \tag{B 1}$$

To leading order, (3.48) and (3.50) for F yield $y_0 = O(\varepsilon^{2/3})$ for $O(|\zeta|) = (4/3)|\ln\varepsilon|$ and, thus,

$$\Sigma \simeq \varepsilon\sqrt{2p_1}. \tag{B 2}$$

Taking into account the next-order term in the expansion of F, ((C 5) in Appendix C), we retrieve (B 1). In the case of non-equilibrium space charge zone ($O(|\zeta|) > (4/3)|\ln\varepsilon|$) (3.56) and (3.61) yield

$$\Sigma = \varepsilon\sqrt{2p_1 + y_0 I} = \frac{\varepsilon}{\sqrt{2p_1}}\left[(y_0 I + 2p_1) + O\left(y_0^2\right)\right].$$

Thus, (B 1) holds for all realistic ζ ($O(|\zeta|) < 1/\varepsilon$. Let us note that for $1/\varepsilon > O(|\zeta|) > 1$ and, respectively, $O(|y_0|) < 1$, (B 2) holds, that is the total charge reaches semi-saturation (for still large $-\zeta = O(1/\varepsilon)$ it will increase further). By integrating the Poissons equation (3.5*b*) in the EDL, we obtain

$$\int_0^{y_1} y(c^+ - c^-)\,\mathrm{d}y = \varepsilon^2\left[-\zeta - \tfrac{2}{3}\ln\varepsilon - \ln(z_1 - z_0)\right], \tag{B 3}$$

where $y_1(z_1)$ is the outer edge defined in § 3.3.2 by Definitions 1 or 2. By using (3.70), and defining the 'centre of charge' in the EDL as

$$Y_\rho \overset{\text{def}}{=} \frac{\int_0^{y_1} y(c^+ - c^-)\,\mathrm{d}y}{\Sigma},$$

and using (B 3), we find

$$Y_\rho \simeq \varepsilon \left[-\frac{\zeta + \frac{2}{3}\ln\varepsilon}{\sqrt{2p_1}} \right], \tag{B 4}$$

for $1/\varepsilon > O(|\zeta|) > (2/3)|\ln\varepsilon|$. Equation (B 4) implies that the 'centre of charge' is moving away from the membrane surface with the increase of $|\zeta|$.

Appendix C. Higher-order terms in the composite Q1DL solution for the critical case $z_0 = O(1)$, $\zeta = O(\frac{4}{3}\ln\varepsilon)$.

Let us rewrite the problem (3.15), (3.17) in terms of the inner thin QE–EDL variables q, Q defined by (3.29a,b)

$$\frac{\mathrm{d}^2\widetilde{Q}}{\mathrm{d}q^2} - \tfrac{1}{2}\widetilde{Q}^3 + z_0\varepsilon^{2/3}\widetilde{Q} - \varepsilon(q\widetilde{Q} + 1) = 0 \quad (0 < q < \infty), \tag{C 1}$$

$$\left(\frac{\mathrm{d}\widetilde{Q}}{\mathrm{d}q} + \tfrac{1}{2}\widetilde{Q}^2\right)\Big|_{q=0} = 2p_1 I^{-2/3} + z_0\varepsilon^{2/3} \quad (\widetilde{Q}|_{q=\infty} = 0). \tag{C 2a,b}$$

Let us seek a solution to the problem (C 1)–(C 2a,b) in the form

$$\widetilde{Q} = Q + \varepsilon^{2/3}Q^{(1)} + \cdots.$$

The leading-order thin QE–EDL solution $Q(q)$ is given by (3.26).

We look for the outer TEDL solution $\widetilde{F}(z)$ to the problem (3.15)–(3.18). Matching with the thin QE–EDL solution yields

$$\widetilde{F}(z) = -\frac{2}{z} + G(z) + \varepsilon^a F^{(1)}(z) + \cdots.$$

Here, $G(z)$ is a solution to the leading-order TEDL problem (3.51), (3.52a,b). The Q1DL solution is a composition of $\varepsilon^{-1/3}\widetilde{Q}\left(z\varepsilon^{-1/3}\right)$ (see (3.29a,b)) and $\widetilde{F}(z)$.

The next-order inner thin QE–EDL problem is

$$\frac{\mathrm{d}^2Q^{(1)}}{\mathrm{d}q^2} = \frac{6}{(q + I^{1/3}\sqrt{2/p_1})^2}Q^{(1)} + \frac{2z_0}{q + I^{1/3}\sqrt{2/p_1}} \quad (0 < q < \infty), \tag{C 3}$$

$$\left(\frac{\mathrm{d}Q^{(1)}}{\mathrm{d}q} - \sqrt{2p_1}Q^{(1)}\right)\Big|_{\widetilde{z}=0} = z_0, \quad Q^{(1)}(\infty) = 0. \tag{C 4a,b}$$

Matching of the solution $Q^{(1)}$ to the thin QE–EDL problem (C 3), (C 4a,b) with the outer TEDL solution $\widetilde{F}(z)$ yields

$$Q^{(1)}(q) = -\frac{\sqrt{2}}{3p_1^{3/2}}\frac{z_0}{(q + I^{1/3}\sqrt{2/p_1})^2} - \frac{z_0}{3}(q + I^{1/3}\sqrt{2/p_1}), \tag{C 5}$$

and

$$\alpha = \tfrac{1}{3}, \quad \widetilde{F}(z) = -\frac{2}{z} + G(z) + \varepsilon^{1/3}\left(\frac{2}{z^2} I^{1/3}\sqrt{\frac{2}{p_1}} + G^{(1)}(z)\right) + \cdots,$$

where $G^{(1)}(z)$ is the regular portion of the next-order term of the outer TEDL solution $F^{(1)}(z)$. $G^{(1)}(z)$ is a bounded solution to the following equation holding for $0 < z < \infty$

$$\frac{\mathrm{d}^2 G^{(1)}}{\mathrm{d}z^2} = \tfrac{3}{2} G^{(1)}\left(G - \frac{2}{z}\right)^2 + 3I^{1/3}\sqrt{\frac{2}{p_1}}\frac{1}{z^2}\left(G^2 - \frac{4}{z}G\right) + (z - z_0)\left(G^{(1)} + \frac{2}{z^2} I^{1/3}\sqrt{\frac{2}{p_1}}\right).$$

Boundedness of $G^{(1)}(z)$ yields the expansion

$$G^{(1)}(z) = \begin{cases} -\dfrac{z_0}{3} I^{1/3}\sqrt{2/p_1} + O(z), & 0 < z \ll 1; \\ -2I^{1/3}\sqrt{2/p_1}[z(z - z_0)]^{-1} + O(z^{-3}), & z \gg 1. \end{cases}$$

Thus, by composing the inner thin QE–EDL solution

$$\widetilde{Q}\left(\frac{z}{\varepsilon^{1/3}}\right) = -\frac{2}{z/\varepsilon^{1/3} + I^{1/3}\sqrt{2/p_1}} - \frac{\sqrt{2} z_0/\varepsilon^{2/3}}{3p_1^{3/2}\left(z/\varepsilon^{1/3} + I^{1/3}\sqrt{2/p_1}\right)^2}$$

$$- \frac{z_0 \varepsilon^{2/3}}{3}\left(\frac{z}{\varepsilon^{1/3}} + I^{1/3}\sqrt{\frac{2}{p_1}}\right) + \cdots$$

with the outer TEDL solution

$$\widetilde{F}(z) = -\frac{2}{z} + G(z) + \varepsilon^{1/3}\left(\frac{2}{z^2} I^{1/3}\sqrt{\frac{2}{p_1}} + G^{(1)}(z)\right) + \cdots$$

and keeping the next-order corrections in the overall composite solution (3.48), we find

$$F_{(0)} + \varepsilon^{1/3} F_{(1)}(z) = -\frac{2}{z + \varepsilon^{1/3} I^{1/3}\sqrt{2/p_1}} + G(z) + \varepsilon^{1/3} G^{(1)}(z).$$

Contribution of higher-order corrections to this composite solution is of the order of $O(\varepsilon^{1/3})$.

Appendix D. Glossary of electrochemical terms

Anion: negative ion.

Bulk electroconvection: electroconvection due to the action of Coulombic forces on a macroscopic scale, as opposed to electro-osmosis, due to the action of the same forces on the Debye length scale of the EDL.

Cation: positive ion.

Concentration polarization (CP): an electrochemical term for a complex of effects related to the formation, under the passage of a transversal electric current, of concentration gradients in electrolyte layers adjacent to a permselective interface (ion exchange membranes, electrode).

Diffusion layer: the part of a viscous boundary layer in which the transversal solute transport is diffusion dominated. In physicochemical applications, the diffusion layer is often modelled as the Nernst film unstirred layer, that is a stagnant fluid

layer, flanked by the solid on one side and the stirred bulk on the other, across which the solute is transferred by diffusion only.

Electric double layer (EDL): a physicochemical term for the boundary layer associated with a small parameter (squared dimensionless Debye length) in the Poisson equation in an electrodiffusional system.

Quasi-equilibrium EDL: the EDL in which the exponential Boltzmann relation holds between the ionic concentration and the electric potential.

EDL polarization: effects of distortion of EDL by the external lateral parameter variation.

Electroconvection (EC): flow of a liquid electrolyte induced by the action of Coulombic forces.

Electrodialysis (ED): desalination and ion separation process, employing ion exchange membrane. The central component of ED is a plain parallel cell formed by anion and cation exchange membranes about 0.1 cm apart. An electrolyte solution is passed through the ED cell while an electric field, is applied transversally from the anion to the cation exchange membranes. Under the action of this field anions and cations migrate towards the respective membranes and leave the cell through them. As a result, the electrolyte concentration at the exit from the cell is reduced compared to that at the entrance.

Electrodiffusion: diffusion of charged particles, combined with their migration in the electric field.

Electrokinetic phenomena: the EDL related flow phenomena, such as electro-osmosis, streaming potential, electrophoresis and sedimentation potential.

Electrolyte, strong: a solution in which the solute (dissolved component) is virtually completely dissociated into cations and anions.

Electro-Osmosis: prototypical electrokinetic effect: generation of a fluid slip due to the action of a lateral Coulombic electric force in the EDL.

Ion exchange membrane: polymer films preferentially permeable to ions of a certain sign. Thus the cation exchange membranes (C-membranes) are practically exclusively permeable only to cations, whereas the anion exchange membrane (A-membrane) are so to anions.

Local electroneutrality approximation: approximate local balance of positive and negative charge carrier concentrations in a macroscopic electrodiffusional system outside the EDL. Mathematically, a property of the outer solution in a singularly perturbed electrodiffusional system with a small parameter in the Poisson equation.

Overlimiting conductance: steady-state passage of an electric current higher than the so-called limiting value through an ion exchange membrane. The following three regions are typically distinguishable in the voltage–current (VC) relation (polarization curve) of an ion exchange membrane (figure 22): the low electric Ohmic region I is followed by a plateau at the limiting current (region II, more pronounced at cation exchange membranes); inflection of the VC curve at the plateau is followed by the overlimiting region III. Transition to region III is accompanied by a threshold appearance of a low-frequency excess electric noise, whose amplitude increases with the distance from the threshold and may reach up to a few per cent of the respective mean value. The mechanisms of the overlimiting conductance and its accompanying excess electric noise remained unclear for a long time. It has been shown conclusively that no such mechanisms as loss of membrane perm-selectivity at high voltage or the appearance of additional charge carriers ("water splitting") are responsible for these phenomena at C-membranes (see Frillete 1957; Block & Kitchener 1966; Simons 1979*a*, *b*; Rubinstein *et al.* 1984). (This is also true for A-membranes, although there the aforementioned overlimiting pattern is obscured because most anion exchange

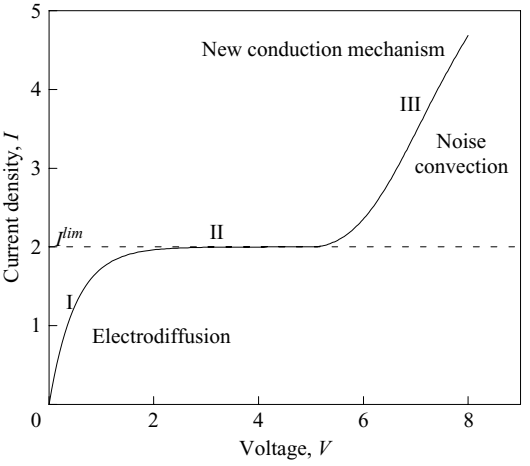

FIGURE 22. Sketch of a typical voltage/current curve of a cation-exchange membrane.

membranes intensely 'split water' in the course of concentration polarization owing to a particular catalytic surface reaction (Simons 1979*a*, *b*; Rubinstein *et al.* 1984). There are a number of indications that the overlimiting behaviour of the C-membranes is associated with some kind of convective mixing that develops spontaneously in the depleted diffusion layer at the advanced stage of CP (see Block & Kitchener 1966; Lifson, Gavish & Reich 1977; Reich, Gavish & Lifson 1978; Li, Fang & Green 1983). This has been finally confirmed by a straightforward experimental finding: if the depleted liquid diffusion layer is replaced by a gel by a gel, a plateau is reached at saturation, and the excess electric noise disappears (Maletzki *et al.* 1992). It was suggested that gravitational convection, brought about by the density gradients due to CP, may destroy the unstirred layer (Lifson *et al.* 1977; Reich *et al.* 1978). It should, however, be remembered that gravitational instability of a laminar sublayer at a smooth solid/liquid interface in a well-mixed bulk flow may occur only upon the fulfilment of quite general hydrodynamic conditions. Whatever the nature of the bulk flow, laminar or turbulent, natural or forced, gravitational instability will destroy an already existing horizontal diffusion layer with a positive upward density gradient (unstable stratification) only if the respective Rayleigh number is above a critical value which is larger than 1000. For an aqueous, 200 μm, or less, thick diffusion layer of a 0.01 or 0.1 normal NaCl solution, the Rayleigh number is 11.6 and 116, respectively, that is at least an order of magnitude below the instability threshold. On the other hand, overlimiting conductance is also observed for a stable density stratification of the depleted diffusion layer (Rubinstein *et al.* 1988, 2002; Maletzki *et al.* 1992; Belova *et al.* 2006). Electroconvection was suggested as an alternative mechanism drawing together the overlimiting phenomena at C-membranes (see Dukhin 1991; Rubinstein 1991; Maletzki *et al.* 1992, Rubinstein, Zaltzman & Kedem 1997).

Perm selectivity: selective permeability för charges of a given sign.

ζ-potential: electric potential drop between the non-slip surface at the solid/liquid interface and the outer edge of the EDL.

REFERENCES

ALEXANDROV, R. S., GRIGIN, A. P. & DAVYDOV, A. P. 2002 Numerical study of electroconvective instability of binary electrolyte in a cell with plane parallel electrodes. *Russ. J. Electrochem.* **38**, 1216–1222.

Baygents, J. C. & Baldessari, F. 1998 Electrohydrodynamic instability in a thin fluid layer with an electrical conductivity gradient. *Phys. Fluids* **10**, 301–311.

Bazant, M. Z. & Squires, T. M. 2004*a* Induced-charge electro-osmosis. *J. Fluid Mech.* **509**, 217–252.

Bazant, M. Z. & Squires, T. M. 2004*b* Induced-charge electrokinetic phenomena: theory and microfluidic applications. *Phys. Rev. Lett.* **92**, 066101.

Bazant, M. Z., Thornton, K. & Ajdari, A. 2004 Diffuse-charge dynamics in electrochemical systems. *Phys. Rev.* E **70**, 021506.

Belova, E. I., Lopatkova, G. Y., Pismenskaya, N. D., Nikonenko, V. V., Larchet, C. & Pourcelly, G. 2006 Effect of anion-exchange membrane surface properties on mechanisms of overlimiting mass transfer. *J. Phys. Chem.* B **110**, 13 458–13 469.

Ben, Y. & Chang, H. C. 2002 Nonlinear Smoluchowski slip velocity and micro-vortex generation. *J. Fluid Mech.* **461**, 229–238.

Block, M. & Kitchener, J. A. 1966 Polarization phenomena in commercial ion-exchange membranes. *J. ElectroChem. Soc.* **113**, 947–953.

Bruinsma, R. & Alexander, S. 1990 Theory of electrohydrodynamic instabilities in electrolytic cells. *J. Chem. Phys.* **92**, 3074–3085.

Buchanan, M. E. & Saville, D. A. 1999 Electrohydrodynamic stability in electrochemical systems. In *Proc. AIChE Annual Meeting* (ed. APS Meeting Abstracts), pp. D8+. Am. Phys. Soc.

Buck, R. P. 1973 Steady-state space-charge effects in symmetric cells with concentration polarized electrodes. *J. Electroanal. Chem.* **46**, 1–23.

Castellanos, A. & Velarde, M. G. 1981 Electrohydrodynamic stability in the presence of a thermal gradient. *Phys. Fluids* **24**, 1784–1786.

Chen, C. H., Lin, H., Lele, S. K. & Santiago, J. G. 2005 Convective and absolute electrokinetic instability with conductivity gradients. *J. Fluid Mech* **524**, 263–303.

Chu, K. T. & Bazant, M. Z. 2005 Electrochemical thin films at and above the classical limiting current. *SIAM J. Appl. Math* **65**, 1485–1505.

Dukhin, S. S. 1991 Electrokinetic phenomena of the second kind and their applications. *Adv. Colloid Interface Sci.* **35**, 173–196.

Dukhin, S. S. & Derjaguin, B. V. 1976 *Electrophoresis*, 2nd edn. Nauka, Moscow (in Russian).

Dukhin, S. S. & Mishchuk, N. A. 1989 Disappearance of limiting current phenomenon in the case of a granule of an ion-exchanger. *Coll. J. USSR* **51**, 570–581 (in Russian).

Dukhin, S. S., Mishchuk, N. A. & Takhistov, P. B. 1989 Electro-Osmosis of the second kind and unrestricted current increase in the mixed monolayer of an ion-exchanger. *Coll. J. USSR* **51**, 616–618 (in Russian).

Fleury, V., Chazalviel, J.-N. & Rosso, M. 1993 Coupling of drift, diffusion, and electroconvection, in the vicinity of growing electrodeposits. *Phys. Rev.* E **48**, 1279–1295.

Fleury, V., Kaufman, J. H. & Hibbert, D. B. 1994 Mechanism of a morphology transition in ramified electrochemical growth. *Nature* **367**, 435–438.

Frillette, V. J. 1957 Electrogravitational transport at synthetic ion exchange membrane surfaces. *J. Phys. Chem.* **61**, 168–174.

Grafov, B. M. & Chernenko, A. A. 1962 Theory of the passage of a constant current through a solution of a binary electrolyte. *Dokl. Akad. Nauk SSSR* **146**, 135–138 (in Russian).

Grigin, A. P. 1985 The convective coulombic instability of binary electrolytes in cells with plane-parallel electrodes. *Sov. Electrochem.* **21**, 48–53.

Grigin, A. P. 1992 Coulomb convection in electrochemical systems. *Sov. Electrochem.* **28**, 247–269.

Helmholtz, H. 1879 Studien uber electrische grenzschichten. *Ann. Phys. Chem.* **7**, 337–382.

Kamin, S., Peletier, L. A. & Vazquez, J. L. 1989 Classification of singular solutions of a nonlinear heat-equation. *Duke Math. J.* **58**, 610–615.

Lerman, I., Rubinstein, I. & Zaltzman, B. 2005 Absence of bulk electroconvective instability in concentration polarization. *Phys. Rev.* E **71**, 011506.

Levich, V. G. 1962 *Physicochemical Hydrodynamics*. Prentice–Hall.

Li, Q., Fang, Y. & Green, M. 1983 Turbulent light scattering fluctuation spectra near a cation electrodialysis membranes. *J. Colloid Interface Sci.* **91**, 412–417.

Lifson, S., Gavish, B. & Reich, S. 1977 Current noise of ion-selective membranes and turbulent convection in the depleted layer. In *Physicochemical Hydrodynamics II* (ed. D. B. Spalding), pp. 141–146. Advance Publications, London.

Listovnichy, A. V. 1989 Passage of currents higher than the limiting one through the electrode–electrolyte solution system. *Elektrokhimia* **25**, 1651–1658 (in Russian).

Livermore, C. & Wong, P. Z. 1994 Convection and turbulence effects in strongly driven electrochemical deposition. *Phys. Rev. Lett.* **72**, 3847–3850.

Maletzki, F., Rosler, H. W. & Staude, E. 1992 Ion transfer across electrodialysis membranes in the overlimiting current range stationary voltage current characteristics and current noise power spectra under different conditions of free convection. *J. Membr. Sci.* **71**, 105–116.

Manzanares, J. A., Murphy, W. D., Mafe, S. & Reiss, H. 1993 Numerical simulation of the nonequilibrium diffuse double layer in ion-exchange membranes. *J. Phys. Chem.* **97**, 8524–8530.

Melcher, J. R. 1981 *Continuum Electromechanics*, 1st edn. MIT Press.

Mishchuk, N., Gonzalez-Caballero, F. & Takhistov, P. 2001 Electro-Osmosis of the second kind and current through curved interface. *Colloids Surfaces* A **181**, 131–144.

Nasumo, S. & Kai, S. 1991 Instabilities and transition to defect turbulence in electrohydrodynamic convection of nematics. *Europhys. Lett.* **14**, 779–783.

Nikonenko, V. V., Zabolotsky, V. I. & Gnusin, N. P. 1989 Electric transport of ions through diffusion layers with impaired electroneutrality. *Sov. Electrochem.* **25**, 262–266.

Perez, A. T. & Castellanos, A. 1989 Role of charge diffusion in finite amplitude electroconvection. *Phys. Rev.* A **40**, 5844–5855.

Posner, J. D. & Santiago, J. G. 2006 Convective instability of electrokinetic flows in a cross-shaped microchannel. *J. Fluid. Mech* **555**, 1–42.

Rehberg, I., Horner, F. & Hartung, G. 1991 The measurement of subcritical electroconvection. *J. Stat. Phys.* **64**, 1017–1023.

Reich, S., Gavish, B. & Lifson, S. 1978 Visualization of hydrodynamic phenomena in the vicinity of a semipermeable membranes. *Desalination* **24**, 295–296.

Reuss, F. F. 1809 Charge-induced flow. *Proc. Imp. Soc. Nat. Moscow* **3**, 327–336.

Rubinstein, I. 1990 *Electrodiffusion of Ions*, 1st edn. SIAM.

Rubinstein, I. 1991 Electroconvection at an electrically inhomogeneous permselective interface. *Phys. Fluids* A **3**, 2301–2309.

Rubinstein, I. & Shtilman, L. 1979 Voltage against current curves of cation exchange membranes. *J. Chem. Soc. Faraday Trans. II* **75**, 231–246.

Rubinstein, I. & Zaltzman, B. 2000 Electro-osmotically induced convection at a permselective membrane. *Phys. Rev.* E **62**, 2238–2251.

Rubinstein, I. & Zaltzman, B. 2001 Electro-osmotic slip of the second kind and instability in concentration polarization at electrodialysis membranes. *Math. Mod. Meth. Appl. Sci.* **11**, 263–300.

Rubinstein, I. & Zaltzman, B. 2003 Wave number selection in a nonequilibrium electro-osmotic instability. *Phys. Rev.* E **68**, 032501.

Rubinstein, I., Warshawsky, A., Schechtman, L. & Kedem, O. 1984 Elimination of acid-base generation ('water splitting') in electrodialysis. *Desalination* **51**, 55–60.

Rubinstein, I., Shtaude, E. & Kedem, O. 1988 Role of the membrane surface in concentration polarization at ion-exchange membrane. *Desalination* **62**, 101–114.

Rubinstein, I., Zaltzman, T. & Zaltzman, B. 1995 Electroconvection in a layer and in a loop. *Phys. Fluids* **7**, 1467–1482.

Rubinstein, I., Zaltzman, B. & Kedem, O. 1997 Electric fields in and around ion-exchange membranes. *J. Membrane Sci.* **125**, 17–23.

Rubinstein, I., Zaltzman, B., Pretz, J. & Linder, C. 2002 Experimental verification of the electroosmotic mechanism of overlimiting conductance through a cation exchange electrodialysis membrane. *Russ. Electrochem.* **38**, 853–864.

Rubinstein, I., Zaltzman, B. & Lerman, I. 2005 Electroconvective instability in concentration polarization and nonequilibrium electro-osmotic slip. *Phys. Rev.* E **72**, 011505.

Saville, D. A. 1997 Electrohydrodynamics: The Taylor–Melcher leaky dielectric model. *Annu. Rev. Fluid Mech.* **29**, 27–64.

Schneider, M. & Watson, P. K. 1970 Electrohydrodynamic stability of space-charge-limited currents in dielectric liquids: I. theoretical study. *Phys. Fluids* **19**, 1948–1954.

Simons, R. 1979*a* The origin and elimination of water splitting in ion-exchange membranes s during water demineralization by electrodialysis. *Desalination* **29**, 41–42.

Simons, R. 1979*b* Strong electric field effects on proton transfer between membrane-bound amines and water. *Nature* **280**, 824–826.

Smoluchowski, M. 1914 *Elektrische Endosmose und Strömungsstr*. J. A. Barth, Leipzig.

Smyrl, W. H. & Newman, J. 1967 Double layer structure at the limiting current. *Trans. Farday Soc.* **63**, 207–216.

Taylor, G. I. 1966 Studies in electrohydrodynamics. i. Circulation produced in a drop byan electric field. *Proc. R. Soc. Lond.* A **291**, 159–166.

Trau, M., Saville, D. A. & Aksay, I. A. 1996 Field-induced layering of colloidal crystals. *Science* **272**, 706–709.

Trau, M., Saville, D.A. & Aksay, I. A. 1997 Assembly of colloidal crystals at electrode interfaces. *Langmuir* **13**, 6375–6381.

Winkler, B. L., Richter, H., Rehberg, I., Zimmermann, W., Kramer, L. & Buka, A. 1991 Nonequilibrium patterns in the electric-field-induced splay fréedericksz transition. *Phys. Rev.* A **43**, 1940–1951.

Zholkovskij, E. K., Vorotyntsev, M. A. & Staude, E. 1996 Electrokinetic instability of solution in a plane-parallel electrochemical cell. *J. Colloid Interface Sci.* **181**, 28–33.